Network Models for Multiobjective Discrete Optimization

David Bergman[*1], Merve Bodur[†2], Carlos Cardonha[‡3], and Andre A. Cire[**4]

[1]Department of Operations and Information Management, University of Connecticut
[2]Department of Mechanical and Industrial Engineering, University of Toronto
[3]IBM Research
[4]Department of Management, University of Toronto Scarborough

September 6, 2018

Abstract

This paper provides a novel framework for solving multiobjective discrete optimization problems with an arbitrary number of objectives. Our framework formulates these problems as *network models*, in that enumerating the Pareto frontier amounts to solving a multicriteria shortest path problem in an auxiliary network. We design techniques for exploiting the network model in order to accelerate the identification of the Pareto frontier, most notably a number of operations to simplify the network by removing nodes and arcs while preserving the set of nondominated solutions. We show that the proposed framework yields orders-of-magnitude performance improvements over existing state-of-the-art algorithms on five problem classes containing both linear and nonlinear objective functions.

Keywords. Multicriteria decision making; multiobjective discrete optimization; dynamic programming; integer programming; Pareto frontier; network models

1 Introduction

Multiobjective optimization is the study of algorithms for optimization problems associated with two or more objective functions. Such problems arise naturally in prescriptive decision making, where decision makers often face conflicting criteria that balance trade-offs associated with a proposed solution. Practical applications of multiobjective optimization are pervasive and found in a diverse set of domains. This includes, for example, production planning for supply chains (Dickersbach 2015), radiotherapy optimization in healthcare (Yu et al. 2000), and aerodynamic design (Wang et al. 2011), which may involve from a few up to potentially hundreds of objective functions. Furthermore, multiobjective optimization can also be used as an alternative method to solve single-objective problems (Bodur et al. 2016), expanding even further on the importance of the study of techniques to tackle these computationally challenging problems.

In this paper, we focus on multiobjective *discrete* optimization problems (MODOs) that admit recursive formulations; in such problems, variables may only assume values from a finite set. There

---

[*]david.bergman@business.uconn.edu

[†]bodur@mie.utoronto.ca

[‡]carloscardonha@br.ibm.com

[**]acire@utsc.utoronto.ca

is a rich history of the study of techniques for addressing MODOs, often leveraging advances in integer programming (IP) technology; see, e.g., in-depth surveys by Ehrgott 2006a and Zhou et al. 2011. Specifically, current state-of-the-art methodologies rely on parametric single-objective reformulations of MODOs, employing commercial IP solvers as black-boxes of their algorithms. The Pareto frontier, however, cannot be fully recovered by such linear parametric models in general (Sayın and Kouvelis 2005). These methods therefore rely on explicit enumeration techniques, limiting the size of problems that can be solved both in terms of the number of variables and the number of objective functions.

Contributions. This paper presents a new approach for modeling and solving MODOs that admit recursive formulations. Our framework reformulates the problem of identifying points in the Pareto frontier as a multicriteria shortest path problem (Garroppo et al. 2010) over a structured network. In particular, the network implicitly represents the objective space in a compact way by exploiting symmetry and dominance relationship between solutions, which can be defined both generally or in a problem-specific form.

Our first contribution is the design of two approaches for obtaining a valid network for a MODO. One is based on a recursive model and the other is extracted from a decision diagram representation of the problem (Bergman et al. 2016). Both techniques leverage construction procedures already available in the literature, some of which are inspired by early dynamic programming (DP) approaches for multiobjective optimization (Carraway et al. 1990). Nonetheless, we exploit the network structure as opposed to the recursive formulation directly, which provides two benefits. First, network representations do not require linear formulations, thereby broadening modeling expressiveness over other popular techniques. Second, network models inherently exploit symmetry by combining subpaths that correspond to common objective function evaluations, decreasing the enumeration requirements from previous techniques.

As our second contribution, we propose *validity-preserving operations* (VPOs) designed to reduce the size of a network while maintaining validity. A network for a MODO is, in general, exponentially large in the input size of the problem. Even if the network itself is of manageable size, computing a multicriteria shortest path may take a prohibitively long time. VPOs simplify the network without modifying the Pareto frontier, leading to significant reductions on the number of arcs and nodes and hence computational time. We explore VPOs that are based solely on the network itself (e.g., removing arcs/nodes, merging nodes) and VPOs that explore domain-specific features of the problem (e.g., using DP state-based information to identify dominance).

Finally, we present an extensive numerical study on five problem classes to compare our network model approach with two state-of-the-art MODO algorithms. We consider the knapsack, set covering, set packing, and the traveling salesperson problem, which are commonly used as benchmarks in the MODO literature, in addition to a MODO with nonlinear terms in the objective motivated from an application in regression-based models.

Our experiments indicate that the proposed approach outperforms the state-of-the-art by orders of magnitude for problem classes where recursive models and state-space relaxations are known to be effective; in particular, the results show a significant expansion on the size of problems that can be solved, specifically in terms of the number of objective functions (up to seven). This is a particularly limiting factor in existing approaches that severely restrict the applicability of multiobjective optimization in real scenarios beyond a few objectives, as highlighted by Duro and Saxena (2017). Examples of applications where the Pareto frontier for four or more objectives is desired include protein structure prediction (Brasil et al. 2013), computational sustainability (Gomes-Selman et al. 2018), storm drainage and work roll cooling (Duro and Saxena 2017), to name a few. In practice, the Pareto frontier fully characterizes the trade-offs among solutions and is post-processed in interactive decision support systems (Stewart et al. 2008). This allows

practitioners to prioritize objectives and operational aspects based on their technical expertise, often on a case-by-case basis, which can be used as opposed to or in conjunction with typical scalarization techniques when multiple objectives are present.

The remainder of this paper is organized as follows. §**??** provides a literature review of MODO, specifically as it relates to the present paper. §2 and §3 formally define MODOs and network models, respectively. §4 describes network construction algorithms. §5 presents VPOs, and §6 presents the multicriteria shortest path algorithms we employ for enumerating the Pareto frontier. §7 describes the results of an experimental evaluation on four problem classes. We conclude and describe future work in §8. Proofs which do not appear in the main text are presented in the appendix, §A.

There is an extensive literature on exact algorithms for generating the Pareto frontier of a MODO. In general, these approaches can be divided into two main classes: those based on *criterion-space search*, and those based on *decision-space search* (Ehrgott et al. 2016, Ehrgott 2006a).

Criterion-space search relies on *scalarizations*, most commonly based on a combination of weighted sums and ϵ-constraints. Weighted-sum methods iteratively solve a single-objective optimization version of the problem where the single objective is defined by various positive-weight combinations of the original objectives. For general MODOs, however, only a portion of the Pareto frontier (those points referred to as *supported* efficient points) can be identified by this approach alone. The remaining points (*unsupported* efficient points) can be found through the ϵ-constraint method, introduced by Haimes et al. (1971), which optimizes one of the original objective functions with the other constraints transformed into parametrized constraints.

Kirlik and Sayın (2014) and Özlen et al. (2014) provide the state-of-the-art criterion-space search algorithms for MODOs with an arbitrary number of objectives. Both algorithms are based on variants of scalarization techniques. These variants build upon the early work by Klein and Hannan (1982), who suggested an iterative approach to generate a subset of the Pareto frontier while refining the search space by the addition of disjunctive constraints. Sylva and Crema (2004) extended this work to an exact algorithm by reformulating the disjunctive conditions as big-M constraints, which was further improved by Lokman and Köksalan (2013) and Bektas (2016). extended to more than two objectives by Tenfelde-Podehl (2003) and further enhanced by Dhaenens et al. (2010). Another generalization of the two-phase method is proposed by Przybylski et al. (2010). Özlen and Azizoğlu (2009), in turn, developed an alternative approach called the *augmented* ϵ-constraint method, which became one of the state-of-the-art methods after later enhancements by Özlen et al. (2014). Another improvement to the augmented ϵ-constraint method is the recursive methodology proposed by Laumanns et al. (2005, 2006), further refined by Kirlik and Sayın (2014) into a computationally practical approach. We note that Boland et al. (2016b) developed an extension of the so-called L-shape search method (specific to triobjective MODOs) that optimizes a linear function over the set of nondominated points, that can also be used to enumerate the Pareto frontier.

Other scalarization methods include the (lexicographic or augmented) weighted Tchebycheff scalarization (Steuer and Choo 1983). The majority of the criterion-space search focuses on *biobjective* problems, where the special structure resulting from only having two objectives can be exploited; see, e.g., Ralphs et al. (2006), Sayın and Kouvelis (2005), Boland et al. (2015), Parragh and Tricoire (2015). Extensions of these ideas have also been proposed for triobjective MODOs, which iteratively decompose the search space into smaller regions, and apply efficient ways to explore and refine these regions (Dächert and Klamroth 2015, Boland et al. 2016a,c).

Decision-space search methods operate over the space defined by the original decision variables. These techniques are typically based on branch-and-bound search developed for mixed-integer linear programs. The first of such algorithms was proposed by Mavrotas and Diakoulaki (1998) for binary MODOs. The algorithm uses an artificial ideal point to define a bounding set, and discovers

nondominated points by solving (via a criterion-space search algorithm) the multiobjective linear programs obtained when all binary variables are fixed. Mavrotas and Diakoulaki (2005) observed that this branch-and-bound in fact generates a superset of the Pareto frontier, and proposed filtering algorithms to eliminate spurious points. Vincent et al. (2013) later showed that the previous algorithm is still incomplete, and proposed a corrected and improved version for biobjective problems. Other branch-and-bound techniques have also been studied by Masin and Bukchin (2008), Sourd and Spanjaard (2008), who suggested enhancements to the bounding aspects.

The first decision-space algorithm for generic MODO based on branch-and-cut was developed by Jozefowiez et al. (2012), where discrete sets are used for lower bounds. Recently, Adelgren and Gupte (2017) developed a new branch-and-bound algorithm which employs multiobjective extensions of many different aspects of branch-and-bound, such as (primal and dual) presolve, preprocessing, node processing, and dual bounding via cutting planes.

Alternative methods that avoid scalarizations are based on DP and implicit enumerative methods for pure binary problems (e.g., Bitran 1977, Bitran and Rivera 1982). DP approaches are typically focused on variants of the multiobjective knapsack problem, such as Villarreal and Karwan (1981) who employed lower and upper bound sets to eliminate dominated solutions. The authors extended their work to general stage-wise separable MODOs (Villarreal and Karwan 1982). Klamroth and Wiecek (2000) presented distinct conceptual DP models for several variants of the multiobjective knapsack problem. Bazgan et al. (2009) developed a new DP approach enhanced with complementary dominance relations for the 0-1 knapsack case. For the biobjective knapsack, Delort and Spanjaard (2010) and Rong and Figueira (2014) proposed a two-phase algorithm and a multiobjective DP algorithm, respectively.

Similar to the above DP approaches, the most relevant works to ours also considered the multiobjective knapsack problem. Captivo et al. (2003) proposed a transformation of biobjective 0–1 knapsack problem into a biobjective shortest path problem, which is solved via an enhanced version of the labeling algorithm for MSPs. Figueira et al. (2010) developed a generic labeling algorithm for the problem that applies existing reformulations from the literature. More recently, state reduction techniques for the biobjective case have been proposed by Rong et al. (2011) and Rong and Figueira (2013), with algorithmic enhancements by Figueira et al. (2013).

2 Multiobjective Discrete Optimization Problems

In this section we present the notation and formalism used throughout the text. For $a \in \mathbb{N}_+$, we let $[a] := \{1, 2, \ldots, a\}$. We denote by $\mathbf{0}$ and $\mathbf{1}$, a vector of zeroes and ones in appropriate dimention, respectively. The notation $\mathbb{B} := \{0, 1\}$ indicates the Boolean set, while the operator $(\cdot)^\top$ denotes the transpose. For a given $v \in \mathbb{R}^p$, we denote the i-th component of v by v_i or $(v)_i$, for all $i \in [p]$.

A multiobjective discrete optimization problem (MODO) is of the form

$$\max \left\{ f(x) := (f_1(x), f_2(x), \ldots, f_K(x)) \, : \, x \in \mathcal{X} \right\}, \tag{$\mathcal{M}$}$$

where $\mathcal{X} \subset \mathbb{Z}^n$, $n \in \mathbb{N}_+$, is a bounded feasible set and $f : \mathcal{X} \to \mathbb{R}^K$ maps each solution $x \in \mathcal{X}$ into a K-dimensional *objective vector* (or image) $y := (f_1(x), \ldots, f_K(x))$, with $f_k : \mathcal{X} \to \mathbb{R}$, $k \in [K]$.

The objective functions are not assumed to have any particular structure, except that they are well-defined in $\mathcal{X}$. For any two objective vectors $y, y' \in \mathbb{R}^K$, we say that y *dominates* y' (or, alternatively, that y' *is dominated by* y), or simply $yx \succ y'$, if (i) $y_k \geq y'_k$ for all $k \in [K]$, and (ii) there exists at least one index $\tilde{k}$ for which $y_{\tilde{k}} > y'_{\tilde{k}}$.

The image defined by the set of feasible solutions is denoted by $\mathcal{Y} := \{f(x) \, : \, x \in \mathcal{X}\}$. An objective vector $y^* \in \mathcal{Y}$ is a *nondominated* point if there exists no other point $y' \in \mathcal{Y}$ for which

$y' \succ y^*$. The set of all nondominated points of $\mathcal{M}$ is denoted by $\mathcal{Y}_N$, also referred to as the *Pareto frontier*. The typical goal of a MODO, and the focus of this paper, is to enumerate $\mathcal{Y}_N$.

Example 1. *We consider a set packing instance as a running example, with $K = 3$:*

$$\max_{x \in \mathbb{B}^7} \quad \big(f_1(x) = 4x_1 + 5x_2 + 3x_3 + 4x_4 + 2x_5 + 1x_6 + 2x_7,$$

$$f_2(x) = 8x_1 + 7x_2 + 1x_3 + 5x_4 + 3x_5 + 3x_6 + 8x_7,$$

$$f_3(x) = 2x_1 + 6x_2 + 8x_3 + 4x_4 + 6x_5 + 5x_6 + 2x_7\big)$$

$$\text{s.t.} \quad x_1 + x_2 + x_3 \le 1, \quad x_2 + x_3 + x_4 \le 1, \quad x_4 + x_5 \le 1,$$

$$x_4 + x_6 \le 1, \quad x_5 + x_7 \le 1, \quad x_6 + x_7 \le 1.$$

The nondominated set $\mathcal{Y}_N$ consists of the four points $y^1 = (6, 7, 19)$, $y^2 = (8, 13, 17)$, $y^3 = (7, 14, 13)$, and $y^4 = (10, 21, 8)$. They are the images, respectively, of the feasible solution vectors $x^1 = (0, 0, 1, 0, 1, 1, 0)$, $x^2 = (0, 1, 0, 0, 1, 1, 0)$, $x^3 = (1, 0, 0, 0, 1, 1, 0)$, and $x^4 = (1, 0, 0, 1, 0, 0, 1)$. □

For any $\bar{\mathcal{Y}} \subseteq \mathcal{Y}$, let $\text{ND}\left(\bar{\mathcal{Y}}\right) := \left\{y \in \bar{\mathcal{Y}} : \nexists\, y' \in \bar{\mathcal{Y}} \text{ with } y' \succ y\right\}$ be an operator that returns the set of vectors within $\bar{\mathcal{Y}}$ that are not dominated by any other vector in the same set. Note that $\mathcal{Y}_N = \text{ND}\left(\mathcal{Y}\right)$. This operator has been studied in the context of relational database systems, where it is known as the *skyline* operator (Borzsony et al. 2001). We refer to the work by Gudala (2012) for a review of algorithms to compute $\text{ND}\left(\cdot\right)$ and their associated complexity analysis. In particular, for $K = 2$, an efficient implementation of $\text{ND}\left(\mathcal{S}\right)$ for a given $\mathcal{S} \subseteq \mathbb{R}^K$ has a worst-case time complexity of $\mathcal{O}(|\mathcal{S}| \log\left(|\mathcal{S}|\right))$. For $K > 2$, it can be efficiently implemented in $\mathcal{O}\left(|\mathcal{S}| \cdot (\log\left(|\mathcal{S}|\right))^{K-2}\right)$.

3   Network Models

This paper proposes the use of *network models* to enumerate $\mathcal{Y}_N$ for a MODO $\mathcal{M}$. In our context, a network model is a layered-acyclic multi-digraph $\mathcal{N} := (\mathcal{L}, \mathcal{A})$ with node set $\mathcal{L}$ and arc set $\mathcal{A}$. Such a model is equipped with specific structure, properties, and attributes associated with $\mathcal{M}$.

The node set $\mathcal{L}$ is partitioned into $n + 1$ non-empty layers $\mathcal{L} := \dot{\bigcup}_{j \in [n+1]} \mathcal{L}_j$. Layers $\mathcal{L}_1$ and $\mathcal{L}_{n+1}$ have cardinality one with $\mathcal{L}_1 := \{\mathbf{r}\}$ and $\mathcal{L}_{n+1} := \{\mathbf{t}\}$. Nodes $\mathbf{r}$ and $\mathbf{t}$ are referred to as the *root* node and the *terminal* node, respectively. The layer index of a node $u \in \mathcal{L}$ is $\ell(u)$, i.e., $u \in \mathcal{L}_{\ell(u)}$. Each arc $a := (r(a), t(a)) \in \mathcal{A}$ is directed from its *arc-root* $r(a) \in \mathcal{L}_j$ to its *arc-terminal* $t(a) \in \mathcal{L}_{j+1}$ for some $j \in [n]$. The layer of an arc is $\ell(a) := \ell(r(a))$. We denote by $\mathcal{A}^+(u) := \{a \in \mathcal{A} : r(a) = u\}$ the set of outgoing arcs from u and by $\mathcal{A}^-(u) := \{a \in \mathcal{A} : t(a) = u\}$ the set of incoming arcs to u.

We define $\mathcal{P}(u, v)$ as the set of arc-specified paths from node u to node v. The arguments will be omitted when $u = \mathbf{r}$ and $v = \mathbf{t}$, i.e., $\mathcal{P} := \mathcal{P}(\mathbf{r}, \mathbf{t})$. Each arc a has an *arc-weight* vector $w(a) \in \mathbb{R}^K$. The arc-weight vectors provide the connection between arc-specified paths in $\mathcal{N}$ and the objective space of $\mathcal{M}$. Any path $p = (a_{j_1}, \ldots, a_{j_H})$ has *path-weight* $w(p) = \sum_{h \in [1, H]} w(a_{j_h})$.

The Pareto frontier of a network model $\mathcal{N}$ is defined as

$$\text{PF}\left(\mathcal{N}\right) := \text{ND}\left(\bigcup_{p \in \mathcal{P}} w(p)\right).$$

A network model $\mathcal{N}$ is *valid* for a MODO $\mathcal{M}$ if $\text{PF}\left(\mathcal{N}\right) = \mathcal{Y}_N$. In our structural results, we may operate on distinct valid network models for the same $\mathcal{M}$, in which case we append a subscript to

our notation so as to indicate the network. For example, $\mathbf{r}_{\mathcal{N}}$ will be used to represent the root node of $\mathcal{N}$. The subscript will be omitted when $\mathcal{N}$ is clear from context.

A network model can be interpreted as a data structure that supports the representation of a MODO $\mathcal{M}$ as a multicriteria shortest path problem (MSP). By negating the arc-weight vectors (since we consider maximization), one may apply any algorithm for solving MSPs to a network model $\mathcal{N}$ in order to find $\mathtt{PF}(\mathcal{N})$ if $\mathcal{N}$ is valid for $\mathcal{M}$. Several MSP algorithms are available; see, e.g., the survey by Garroppo et al. (2010).

Example 2. *Figure 1 depicts a network model $\mathcal{N}$ for the MODO in Example 1. The arc-weight vectors are shown (in black text) next to each arc (the additional details provided in the figure, in red and blue, will be introduced and described in Example 6). There are 14 arc-directed paths from $\mathbf{r}$ to $\mathbf{t}$, and their path-weights are given by*

$$\bigcup_{p \in \mathcal{P}} w(p) = \big\{ (8,13,17), (6,10,11), (7,15,8), (6,7,19), (4,4,13), (5,9,10), (3,6,11),$$

$$(1,3,5), (2,8,2), (7,14,13), (6,13,6), (5,11,7), (6,16,4), (10,21,8) \big\}$$

and results in

$$\mathtt{PF}(\mathcal{N}) = \mathtt{ND}\left(\bigcup_{p \in \mathcal{P}} w(p)\right) = \big\{ (8,13,17), (6,7,19), (7,14,13), (10,21,8) \big\}.$$

$\square$

4 Network Model Construction

This section provides two frameworks for constructing valid network models for MODOs. The first approach relies on a recursive model of $\mathcal{M}$. The second is a direct transformation from decision diagrams, which is applicable when the objective functions are additively separable.

4.1 Recursive Formulations

Several classes of single-objective optimization problems admit recursive formulations, often written as DP models (Bertsimas and Tsitsiklis 1997). These ideas were extended to the case of multiple objectives in the early work by Villarreal and Karwan (1982), which we build upon in this paper. In particular, while DP models are intrinsically associated with a state-transition graph, we show that multiobjective recursive formulations are analogously associated with a valid network model.

Formally, a multiobjective recursive formulation of a MODO $\mathcal{M}$ is written in terms of the following elements as depicted in Figure 2: (i) $n+1$ state variables $s_0, s_1, \ldots, s_n \in \mathcal{S}$ for some state space $\mathcal{S} \subseteq \mathbb{R}^m$, where the initial state s_0 is fixed; (ii) n functions $\mathcal{V}_1, \ldots, \mathcal{V}_n : \mathcal{S} \to 2^{\mathbb{Z}}$ that represent the variable-value assignments that can be applied at a state (i.e., they provide state-dependent feasible decisions); (iii) n state transition functions $\tau_1, \ldots, \tau_n : \mathcal{S} \times \mathbb{Z} \to \mathcal{S}$, each mapping a pair (s, x) of a state $s \in \mathcal{S}$ and a variable-value assignment $x \in \mathbb{Z}$ to another state $s' \in \mathcal{S}$; and (iv) n reward functions $\delta_1, \ldots, \delta_n : \mathcal{S} \times \mathbb{Z} \to \mathbb{R}^K$ that map an analogous pair (s, x) to a reward vector in $\mathbb{R}^K$.
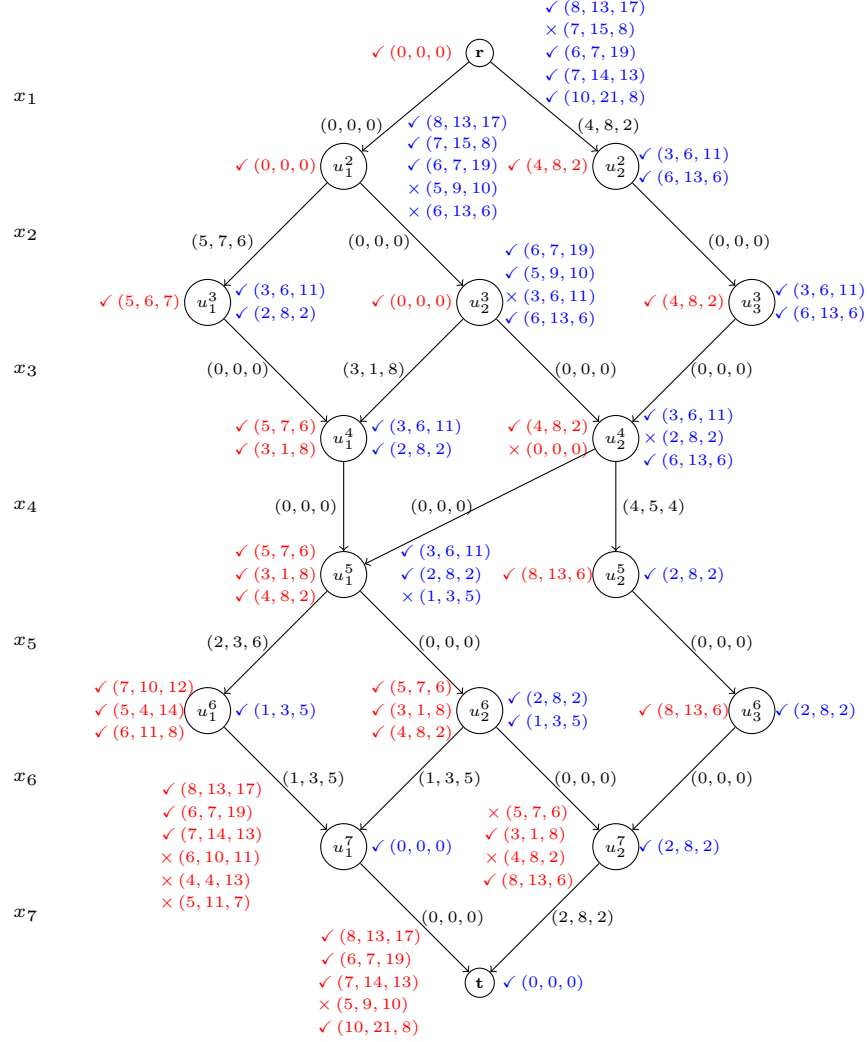
Figure 1: A valid network model for $\mathcal{M}$ in Example 1.

Based on these four components, a multiobjective recursive problem is of the form

$$\max_{s,x} \quad \sum_{j=1}^{n} \delta_j(s_{j-1}, x_j) \tag{$\mathcal{M}_\mathcal{R}$}$$

$$\text{s.t.} \quad s_j = \tau_j(s_{j-1}, x_j), \qquad \text{for all } j \in [n],$$

$$\qquad x_j \in \mathcal{V}_j(s_{j-1}), \qquad \text{for all } j \in [n].$$

In particular, each objective function evaluation is represented by the k-th index of the total reward tuple $\sum_{j=1}^{n} \delta_j(s_{j-1}, x_j)$ for $k \in [K]$, i.e.,

$$f_k(s, x) := \left(\sum_{j=1}^{n} \delta_j(s_{j-1}, x_j) \right)_k,$$

while the feasible set of $\mathcal{M}_\mathcal{R}$ is

$$\mathcal{X} := \left\{ (s, x) \in \mathcal{S}^{n+1} \times \mathbb{Z}^n \; : \; s_j = \tau_j(s_{j-1}, x_j), \; x_j \in \mathcal{V}_j(s_{j-1}) \quad \text{for all } j \in [n] \right\}.$$
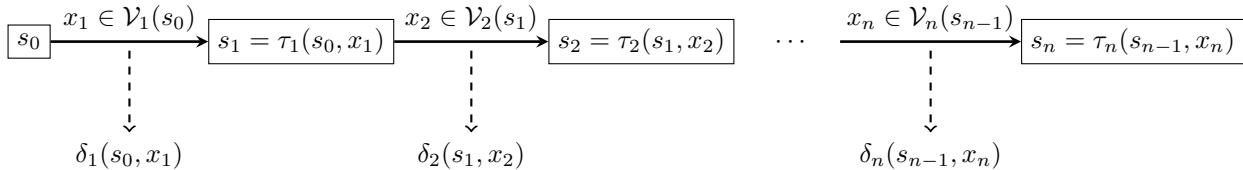
Figure 2: Elements of a recursive formulation

Assume, without loss of generality, that $\tau_n(s,x) = s_{\mathbf{t}}$ for a fixed $s_{\mathbf{t}}$ and for all $s \in \mathcal{S}$, $x \in \mathbb{Z}$. That is, the final transition always leads to a common *terminal* state $s_{\mathbf{t}}$, which can always be accomplished by appropriately defining $\tau_n(\cdot)$. If a MODO can be written in the form of $\mathcal{M}_{\mathcal{R}}$, it exposes a recursive structure that can be immediately leveraged for the construction of a network model. More specifically, the network $\mathcal{N} = (\mathcal{L}, \mathcal{A})$ is the state-transition graph defined by the feasible set $\mathcal{X}$, which is composed as follows (see, e.g., Bertsekas 2017 for algorithmic details):

- Node set $\mathcal{L}$: The nodes of $\mathcal{N}$ are associated with nodes of the state-transition graph. For any $j \in [n+1]$, there exists a node $u \in \mathcal{L}_j$ for every possible value of the state variable s_{j-1} in $\mathcal{X}$. More specifically, at layer j of $\mathcal{N}$, there exists one node for each state in the set $\text{Proj}_{s_{j-1}}(\mathcal{X})$, defined as the projection of the feasible set $\mathcal{X}$ into the space of the variable s_{j-1}. With a slight abuse of notation, we let $\mathcal{L}_j = \{u_1^j, \ldots, u_{|\mathcal{L}_j|}^j\} = \text{Proj}_{s_{j-1}}(\mathcal{X})$. Note that since s_0 and $s_{\mathbf{t}}$ are fixed, layers $\mathcal{L}_1$ and $\mathcal{L}_{n+1}$ are singletons; namely $u_1^1 = s_0$ and $u_1^{n+1} = s_{\mathbf{t}}$.

- Arc set $\mathcal{A}$: The arcs of $\mathcal{N}$ are associated with arcs of the state-transition graph. In other words, there exists an arc in $\mathcal{N}$ for every possible transition in the state-transition graph. Again with a slight abuse of notation, we represent an arc as a triplet, rather than a pair, $(r(a), t(a), x)$ appending the variable-value information. Then, we have

$$\mathcal{A} = \bigcup_{j \in [n]}^{\cdot} \left\{ (u_i^j, u_{i'}^{j+1}, x) : u_i^j \in \mathcal{L}_j,\ u_{i'}^{j+1} \in \mathcal{L}_{j+1},\ x \in \mathcal{V}_j(u_i^j) \text{ with } u_{i'}^{j+1} = \tau_j(u_i^j, x) \right\}.$$

- Arc weights: The reward functions provide the arc weights for $\mathcal{N}$. That is, if $a = (u_i^j, u_{i'}^{j+1}, x) \in \mathcal{A}$, then $w(a) = \delta_j(u_i^j, x)$.

It follows from the definition of arc weights that a path weight corresponds to the objective function in $\mathcal{M}_{\mathcal{R}}$ and, by construction of the state-transition graph, that there is a one-to-one mapping between paths of $\mathcal{N}$ and solutions in $\mathcal{X}$. Thus, $\mathcal{N}$ is a valid network model for $\mathcal{M}_{\mathcal{R}}$.

Example 3. *The instance in Example 1 is a set packing instance, so it can be written as*

$$\max \left\{ \left((c^1)^\top x, (c^2)^\top x, \ldots, (c^K)^\top x \right) : Ax \leq \mathbf{1}, x \in \mathbb{B}^n \right\}$$

for an $m \times n$ matrix A with elements $a_{ij} \in \mathbb{B}^n$, $i \in [m], j \in [n]$, and cost vectors $c^j \in \mathbb{R}^n$, $j \in [n]$.

A recursive formulation can be obtained as follows. A state variable $s \in \mathbb{B}^m$ is defined so that for any $i \in [m]$, $s_i = 1$ if and only if the i-th constraint of $Ax \leq \mathbf{1}$ is satisfied as an equality or all the decision variables appearing in the constraint have already been assigned to zero. Therefore, we have the initial state $s_0 = \mathbf{0}$, whereas any final transition will lead to the terminal state $s_{\mathbf{t}} = \mathbf{1}$. Variable-value assignments $x_j \in \mathbb{B}$ represent the packing of element j. We are not allowed to set a variable $x_j = 1$ if any constraint which includes x_j holds as an equality; i.e.,

$$\mathcal{V}_j(s) := \{b \in \mathbb{B} \ : \ s_i + b \leq 1 \text{ for all } i \in [m] \text{ with } a_{ij} = 1\}.$$

8

The transition function ensures the consistency of the current state s and the next state $\tilde{s}$ when setting $x_j = b$, $b \in \mathcal{V}_j(s)$. Specifically, let $m_i := \arg\max\{j \in [n] : a_{ij} = 1\}$ be the maximum index of the variables with a nonzero coefficient in the i-th constraint. Then, we have $\tau_j(s, b) = \tilde{s}$ where

$$\tilde{s}_i = \begin{cases} 1, & \text{if } j = m_i \\ s_i + b, & \text{if } j < m_i \text{ and } a_{ij} = 1 \qquad \text{for all } i \in [m], \\ s_i, & \text{otherwise} \end{cases}$$

for any $j \in [n]$. Finally, the reward function for each $j \in [n]$ is the contribution of x_j to the objective function vector, which in this particular instance is state independent: $\delta_j(s, b) := b \times \left(c_j^1, c_j^2, \ldots, c_j^K \right)$.

For our particular instance in Example 1, this recursive formulation yields the network model depicted in Figure 15 in the appendix. We note that this network model matches the one given in Figure 1 until layer six (inclusive). The network model in Figure 1 can be obtained from the one in Figure 15 after applying Theorem 1 and Corollary 1 on layer seven. $\qquad\square$

4.2 Transformation from Decision Diagrams

A decision diagram (DD) is a network-based representation of a Boolean or a discrete function with a large list of applications in mathematical programming, operations research, and circuit design (see, e.g., Bryant 1992, Behle 2007, Hadzic and Hooker 2007, Bergman et al. 2011). In such applications, DDs are used to compactly represent or approximate the set of feasible solutions to a discrete optimization problem. We refer to the work by Bergman et al. (2016) for a survey of concepts and existing DD methodologies for optimization.

Each layer in a DD $\mathcal{D}$, except the last one, corresponds to a unique decision variable mapped via the bijective function $y : [n] \to [n]$; that is, layer $l \in [n]$ corresponds to variable $x_{y(l)}$. Let $\mathcal{P}_\mathcal{D}$ be the set of paths from root to terminal in $\mathcal{D}$. The arc-domains associate each path $p = (a_1, \ldots, a_n)$ in $\mathcal{P}_\mathcal{D}$ with a solution vector $x(p) \in \mathbb{Z}^n$ defined by $x(p)_{y(\ell(a_j))} = d(a_j)$ for all $j \in [n]$. In particular, for a given feasible set $\mathcal{X} \subset \mathbb{Z}^n$, $\mathcal{D}$ is said to be *exact* for $\mathcal{X}$ if and only if $x(p) \in \mathcal{X}$ for all $p \in \mathcal{P}_\mathcal{D}$ and $|\mathcal{P}_\mathcal{D}| = |\mathcal{X}|$. That is, the paths of $\mathcal{D}$ encode $\mathcal{X}$ exactly. In summary, decision diagrams are closely related to network models, but observe that arc-domains are exclusive to the former whereas arc-weight vectors it is are defined only in the latter.

Assume that, for a given MODO $\mathcal{M}$, the objective function $f_k(\cdot)$ is separable for all $k \in [K]$; i.e.,

$$f_k(x) := \sum_{j \in [n]} f_{k,j}(x_j)$$

for an appropriate choice of functions $f_{k,j} : \mathbb{Z} \to \mathbb{R}$, $j \in [n]$. In that case, we can transform an exact DD representing $\mathcal{M}$ into a network model $\mathcal{N}$ simply by defining suitable arc weights and removing the arc-domain labels. More specifically, for every arc $a \in \mathcal{A}$, we define its weight according to the variable corresponding to the layer of that arc, $x_{y(\ell(a))}$, and its assigned value, $d(a)$, as $w(a) := \left(f_{1,y(\ell(a))}(d(a)), \ldots, f_{K,y(\ell(a))}(d(a)) \right)$. The assignment of those weights to arcs implies that, for any path $p = (a_1, \ldots, a_n)$ in the network,

$$w(p) = \sum_{j \in [n]} \left(f_{1,y(\ell(a_j))}(d(a_j)), \ldots, f_{K,y(\ell(a_j))}(d(a_j)) \right) = f(x(p)),$$

thus $\mathsf{PF}(\mathcal{N})$ is the Pareto frontier of $\mathcal{M}$. This relation was first used in Bergman and Cire (2016).

There exists an extensive number of DD construction algorithms for discrete optimization problems with a (single) separable objective function (Bergman et al. 2016), some of which will be

employed for our numerical study in Section 7. Note, however, that our proposed network models, after modifications by VPOs, do not necessarily map to valid exact DDs. Indeed, our network operators are guaranteed only to preserve the Pareto frontier, and as such the diagram is typically modified to readjust weights, merge nodes, include infeasible paths, or exclude feasible paths to allow for smaller network sizes (hence not satisfying the basic properties of an exact DD).

As mentioned in Example 3, our running Example 1 is a set packing instance. §4 of Bergman et al. (2016) provides a DD representation for the set packing problem that can be readily transformed into a network model by applying the methodology described above.

5   Validity-preserving Operations

This section is devoted to the study of generic algorithms, denoted by validity preserving operations (VPOs), to transform a network $\mathcal{N}$ into a smaller network $\mathcal{N}'$ such that $\mathrm{PF}\left(\mathcal{N}\right) = \mathrm{PF}\left(\mathcal{N}'\right)$. For the structural results below, we assume that an initial valid network model $\mathcal{N} = \left(\mathcal{L}, \mathcal{A}\right)$ is available.

5.1   Weight Shifting and Node Merging

We extend the classical concept of *reduction* proposed by Bryant (1986) as a VPO for network models. Reduction is an operation applied to DDs that merge nodes which share isomorphic subgraphs. Hooker (2013) later extended this notion for DPs with state-dependent rewards, showing that further merging can be achieved for single-objective problems by considering isomorphism with respect to arc weights.

Based on this concept, we define a weight-shifting operation that, given a node u, transfers weights from the arcs directed out of u (i.e., $\mathcal{A}^+(u)$) to those directed into u (i.e., $\mathcal{A}^-(u)$).

Proposition 1 (Weight shift). *Let $u \in \mathcal{L}$ be a node in $\mathcal{N}$ such that $u \notin \{\mathbf{r}, \mathbf{t}\}$. For any $\tilde{c} \in \mathbb{R}^K$, the operations defined by (1) and (2) below is a VPO:*

1. *$w\left(a\right) := w\left(a\right) - \tilde{c}$ for all $a \in A^+(u)$; and*

2. *$w\left(a\right) := w\left(a\right) + \tilde{c}$ for all $a \in A^-(u)$.*

Proof. Arc-weight $w(p)$ remains unchanged for all $p \in \mathcal{P}$ and thus $\mathrm{PF}\left(\mathcal{N}\right)$ is unchanged. □

Example 4. *Consider the network model in Figure 1. Let $\tilde{c} = (2, 8, 2)$. The network model resulting from subtracting $\tilde{c}$ from arc-weight $w\left(u_2^7, \mathbf{t}\right)$ and adding $\tilde{c}$ to arcs $w\left(u_2^6, u_2^7\right)$ and $w\left(u_3^6, u_2^7\right)$ corresponds to the operations in Proposition 1. The last three layers of $\mathcal{N}$ are reproduced in Figure 3. The result of applying the weight shift is depicted in Figure 4.* □

We now present a sufficient condition for when merging nodes is a VPO.

Theorem 1 (Node merge). *Let $u_1, u_2 \in \mathcal{L}$, $u_1 \neq u_2$, be two nodes in $\mathcal{N}$ for which there exists a one-to-one mapping between the arcs in $\mathcal{A}^+(u_1)$ and $\mathcal{A}^+(u_2)$ satisfying that, for every pair of arcs (a_1, a_2) such that $a_1 \in \mathcal{A}^+(u_1)$ maps to $a_2 \in \mathcal{A}^+(u_2)$, we have $t\left(a_1\right) = t\left(a_2\right)$ and $w(a_1) = w(a_2)$. Then, the following sequence of operations characterizes a VPO:*

1. *Delete all arcs in $\mathcal{A}^+(u_2)$;*

2. *Redefine $t\left(a\right) = u_1$ for all $a \in \mathcal{A}^-(u_2)$; and*
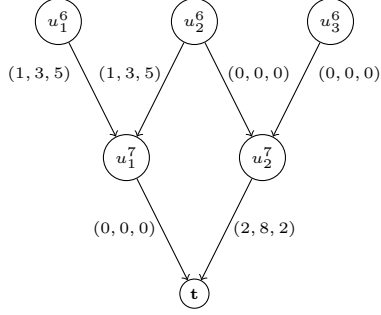
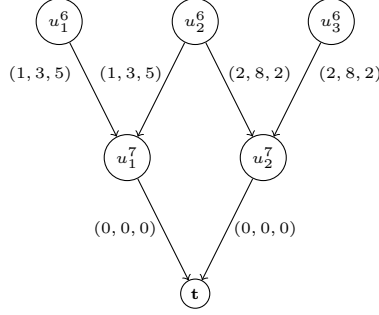3. *Delete u_2,*

10

Figure 3: Original arc-weights

Figure 4: Weight shift by $\tilde{c} = (2, 8, 2)$ at node u_2^7
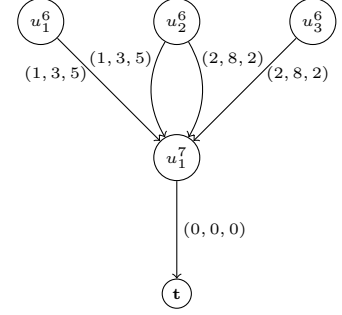
Figure 5: Result of merge operation on nodes u_1^7 and u_2^7

Example 5. *Figure 5 depicts the result of merging nodes u_1^7 with u_2^7 in Figure 4. Note that the resulting network model has fewer arcs and nodes, but the same number of paths. Such an operation thereby decreases the size of the network model without altering* $\mathtt{PF}(\mathcal{N})$. $\qquad\square$

Proposition 1 and Theorem 1 define a strategy for simplifying a network model. In particular, starting from the penultimate layer and moving upwards in the network, we process each node in the layer in the following way. We construct the vector $\tilde{c}(u)$ for each node u in the inspected layer by taking the component-wise minimum arc-weight among arcs in $\mathcal{A}^+(u)$. Once $\tilde{c}(u)$ has been obtained, the arc-weights are shifted up as prescribed in Proposition 1. After repeating this operation to all nodes in a layer, the conditions of Theorem 1 and its VPO are applied to the nodes of the same layer in the transformed network. Node-merge operations can be performed in any order, in the sense that any sequence will lead to the same reduced network.

Proposition 2. *The component-wise minimum arc-weight shift and node merge VPO have worst-case time complexity of* $\mathcal{O}(K|\mathcal{L}|^2 \log(|\mathcal{L}|))$.

5.2 Arc removal

In this section, we investigate algorithms and structural results of VPOs that eliminate arcs of the network model. For an arc $a \in \mathcal{A}$, let $\mathcal{N} - a$ be the network model resulting from the removal of a from $\mathcal{N}$. By definition, removing arc a is a VPO if and only if $\mathtt{PF}(\mathcal{N}) = \mathtt{PF}(\mathcal{N} - a)$. The following theorem shows that identifying when such condition holds in general is an NP-Hard problem.

Theorem 2. *Given a valid network model $\mathcal{N} = (\mathcal{L}, \mathcal{A})$ for a MODO $\mathcal{M}$, let $\tilde{\mathcal{A}} \subseteq \mathcal{A}$ be a subset of arcs of $\mathcal{N}$. Deciding whether there exists an arc $a \in \tilde{\mathcal{A}}$ such that $\mathtt{PF}(\mathcal{N}) = \mathtt{PF}(\mathcal{N} - a)$ is NP-hard.*

Despite the hardness of determining whether an arc can be safely removed without changing the Pareto frontier, we can still exploit strong sufficient conditions for designing arc-removal VPOs. Additional notation is in order. Given a network model $\mathcal{N} = (\mathcal{L}, \mathcal{A})$ and two nodes $u, v \in \mathcal{L}$ such that $\ell(u) < \ell(v)$, let $\mathcal{N}[u, v]$ be the network model containing only nodes and arcs in $\mathcal{N}$ that lie on some path which starts at node u and ends at node v. We introduce the following concept:

Definition 1. *A pair of nodes $u, v \in \mathcal{L}$ is* isolating *in $\mathcal{N}$ when, for every arc $a \in \mathcal{A}_{\mathcal{N}} \backslash \mathcal{A}_{\mathcal{N}[u,v]}$,*

(i) $t(a) \in \mathcal{L}_{\mathcal{N}[u,v]}$ implies that $t(a) = u$; and

(ii) $r(a) \in \mathcal{L}_{\mathcal{N}[u,v]}$ implies that $r(a) = v$.

11

According to Definition 1, nodes u and v are isolating in $\mathcal{N}$ if $\mathcal{N}[u,v]$ contains all arcs from $\mathcal{N}$ that are directed to nodes in $\mathcal{L}_{\mathcal{N}}[u,v]\backslash\{u\}$ and all arcs that are directed out of nodes in $\mathcal{L}_{\mathcal{N}}[u,v]\backslash\{v\}$. (For example, any pair of nodes are isolating in Figure 14(a).) Note that one can check whether two nodes u and v are isolating in $\mathcal{N}$ in polynomial time, in the size $\mathcal{N}$, with a breadth-first search.

Pairs of isolating vertices yield a sufficient condition for an arc-removal operation to be a VPO.

Theorem 3. *Let u and v be isolating nodes in a network model $\mathcal{N}$. For any $a \in \mathcal{A}_{\mathcal{N}[u,v]}$, if $\mathrm{PF}\left(\mathcal{N}[u,v]\right) = \mathrm{PF}\left(\mathcal{N}[u,v]-a\right)$, then $\mathrm{PF}\left(\mathcal{N}\right) = \mathrm{PF}\left(\mathcal{N}-a\right)$. That is, if the removal of arc a is a VPO in $\mathcal{N}[u,v]$, then it is also a VPO in $\mathcal{N}$.*

The proof of Theorem 3 is provided in Section A.4.

Theorem 3 shows that pairs of isolating nodes in an arbitrary network model $\mathcal{N}$ define subnetworks whose VPOs involving the removal of arcs are also VPOs for $\mathcal{N}$. The simplest case reduces to two arcs with the same endpoints, which yields the following immediate corollary.

Corollary 1. *Let a_1 and a_2 be any two arcs of a network model $\mathcal{N}$ for which $r\left(a_1\right) = r\left(a_2\right)$ and $t\left(a_1\right) = t\left(a_2\right)$. If $w\left(a_1\right) \prec w\left(a_2\right)$ or $w\left(a_1\right) = w\left(a_2\right)$, then the removal of a_1 is a VPO.*

Theorem 3 can also be applied directly by choosing two nodes u, v such that $N[u,v]$ is sufficiently small so that all associated arcs can be removed efficiently. Specifically, given $\Delta := \ell\left(v\right) - \ell\left(u\right)$, the number of paths in $\mathcal{N}[u,v]$ is bounded by $\mathcal{O}(2^{\Delta})$, and hence for small Δ the Pareto frontier (and arc to be removed) can be identified quickly using, e.g., the procedures from Section 6, which we discuss next. For our numerical evaluation, we fixed $\Delta = 2$. That is, (i) we find a pair (u,v) of isolating nodes that are distant by at most two layers, (ii) obtain the network model $\mathcal{N}[u,v]$, (iii) compute its Pareto frontier, and finally (iv) apply Theorem 3 to remove arcs that are VPOs in $\mathcal{N}$.

6 Generating the Pareto Frontiers from a Network Model

Given a valid network model, finding the Pareto frontier generally reduces to solving an MSP (by multiplying arc-weights by -1) in a layered-acyclic multi-digraph, for which an extensive literature exists; see, e.g., surveys by Tarapata 2007 and Garroppo et al. 2010.

In this section, we propose two methodologies for enumerating the Pareto frontier based on our network model structure. The first is a direct modification of the unidirectional recursion by Henig (1986), also applied, e.g., in Figueira et al. (2013) and Rong and Figueira (2014). The second technique is an extension of Galand et al. (2013) and performs a bidirectional search that combines the partial Pareto frontiers of each layer using a *coupling* operator. Both methodologies assign a set (or a collection of sets) of K-dimensional vectors to nodes of the network. Each K-dimensional vector is henceforth referred to as a *label*, as is done in the MSP literature.

6.1 Unidirectional Pareto frontier generation

The unidirectional algorithms process one layer at a time, computing the partial nondominated solutions at a node based on either the incoming arcs or the outgoing arcs. It is a direct application of the recursion by Henig (1986) but using the underlying structure of the network model, similar to the version presented by Rong and Figueira (2014).

The procedure works as follows. When processed from the root node $\mathbf{r}$ to the terminal node $\mathbf{t}$, the algorithm assigns a single set of *top-down labels* $\mathcal{Z}^{\mathrm{TD}}\left(u\right)$ to each node u. The label set of each node is initialized as the empty set, except the root node, where $\mathcal{Z}^{\mathrm{TD}}\left(\mathbf{r}\right)$ is initialized as $\{\mathbf{0}\}$. For each layer j from one to n, having constructed $\mathcal{Z}^{\mathrm{TD}}\left(u\right)$ for all $u \in \mathcal{L}_j$, the labels are constructed

for the nodes in $\mathcal{L}_{j+1}$ by considering the arcs directed from nodes in $\mathcal{L}_j$ to $\mathcal{L}_{j+1}$, one by one. For each such arc a (i.e., $a \in \bigcup_{u \in \mathcal{L}_j} \mathcal{A}^+(u)$) and every label $z \in \mathcal{Z}^{\mathrm{TD}}(r(a))$, the label $z + w(a)$ is added to $\mathcal{Z}^{\mathrm{TD}}(t(a))$. After all arcs directed out of nodes in $\mathcal{L}_j$ are processed, $\mathcal{Z}^{\mathrm{TD}}(u)$ is re-assigned to $\mathrm{ND}\left(\mathcal{Z}^{\mathrm{TD}}(u)\right)$, to remove any labels that are dominated by other labels in the set. Note that one can also do a simple check each time a label is added to see if it is dominated by another label already existing for the node. At the culmination of the algorithm, $\mathcal{Z}^{\mathrm{TD}}(\mathbf{t})$ will be $\mathrm{PF}(\mathcal{N})$.

One can also run the algorithm in the opposite direction, starting from $\mathbf{t}$ and flipping the direction of the arcs. The terminal node is initialized as $\{\mathbf{0}\}$, and the nodes are processed in the opposite direction. We refer to the labels constructed in this direction as *bottom-up labels* $\mathcal{Z}^{\mathrm{BU}}(u)$. The set of labels $\mathcal{Z}^{\mathrm{BU}}(\mathbf{r})$ coincides with $\mathcal{Z}^{\mathrm{TD}}(\mathbf{t})$ and is therefore equal to $\mathrm{PF}(\mathcal{N})$.

Example 6. *Consider Figure 1. The labels on the left of the nodes (shown in red) correspond to the top-down labels (i.e., for every node u, they list $\mathcal{Z}^{\mathrm{TD}}(u)$). A "✓" is drawn next to labels that remains in $\mathcal{Z}^{\mathrm{TD}}(u)$ after the application of the $\mathrm{ND}()$ operator, and a "×" is drawn otherwise. To the right of each node u, $\mathcal{Z}^{\mathrm{BU}}(u)$ is listed (in blue), with symbols "✓" and "×" indicating whether the labels remain or are discarded after the application of the $\mathrm{ND}()$ operator, respectively.* □

6.2 Bidirectional Pareto frontier generation

We now provide a compilation method that extends the work of Galand et al. (2013) for network models. Namely, one may obtain the elements composing the Pareto frontier by constructing labels in both directions simultaneously and *coupling* the top-down and bottom-up labels. Given two sets of vectors $\mathcal{Z}_1, \mathcal{Z}_2 \subseteq \mathbb{R}^K$, define the coupling of $\mathcal{Z}_1$ and $\mathcal{Z}_2$ as

$$\mathrm{CP}(\mathcal{Z}_1, \mathcal{Z}_2) := \mathrm{ND}\left(\left\{z : z = z^1 + z^2, z^1 \in \mathcal{Z}_1, z^2 \in \mathcal{Z}_2\right\}\right).$$

The coupling function $\mathrm{CP}(\mathcal{Z}_1, \mathcal{Z}_2)$ returns the nondominated set of vectors that result from every pairwise sum of vectors from the two sets $\mathcal{Z}_1$ and $\mathcal{Z}_2$.

Let us fix a layer j' and suppose we created the labels $\mathcal{Z}^{\mathrm{TD}}(u)$ for every node $u \in \mathcal{L}_j$, $j \leq j'$, and the labels $\mathcal{Z}^{\mathrm{BU}}(u)$ for every node $u \in \mathcal{L}_j$, $j \geq j'$. We define the operation of *coupling on layer j'* as

$$\mathrm{CP}^{\mathrm{L}}(\mathcal{L}_{j'}) := \mathrm{ND}\left(\bigcup_{u \in \mathcal{L}_{j'}} \mathrm{CP}\left(\mathcal{Z}^{\mathrm{TD}}(u), \mathcal{Z}^{\mathrm{BU}}(u)\right)\right).$$

This yields the nondominated set that results from the coupling of the top-down and the bottom-up labels on each node. Note that $\mathrm{CP}^{\mathrm{L}}(\mathcal{L}_j) = \mathcal{Y}_{\mathrm{N}}$ for any $j \in [n+1]$.

Example 7 shows that this approach can significantly reduce the number of operations required to find the Pareto frontier of a network model. Since the nondominated frontier of any set $\mathcal{S}$ of K-dimensional vectors can be found in time $\mathcal{O}\left(|\mathcal{S}| \cdot (\log(|\mathcal{S}|))^{K-2}\right)$ (Borzsony et al. 2001), the coupling operation of sets Z_1 and Z_2 can be completed in time $\mathcal{O}\left(|\mathcal{Z}_1| \cdot |\mathcal{Z}_2| \cdot (\log(|\mathcal{Z}_1| \cdot |\mathcal{Z}_2|))^{K-2}\right)$.

Example 7. *Consider the network model in Figure 1. Suppose we fix $\mathcal{L}_5$, composed of nodes u_1^5 and u_2^5, as the coupling layer. Only 14 top-down labels need to be created to find $\mathcal{Z}^{\mathrm{TD}}(u_1^5)$ and $\mathcal{Z}^{\mathrm{TD}}(u_2^5)$, and only 11 bottom-up labels need to be created in order to find $\mathcal{Z}^{\mathrm{BU}}(u_1^5)$ and $\mathcal{Z}^{\mathrm{BU}}(u_2^5)$. The coupling of these sets results in*

$$\begin{aligned} \mathrm{CP}\left(\mathcal{Z}^{\mathrm{TD}}(u_1^5), \mathcal{Z}^{\mathrm{BU}}(u_1^5)\right) &= \{(8,13,17), (6,7,19), (7,14,13), (7,15,8), (6,16,4)\} \\ \mathrm{CP}\left(\mathcal{Z}^{\mathrm{TD}}(u_2^5), \mathcal{Z}^{\mathrm{BU}}(u_2^5)\right) &= \{(10,21,8)\}, \end{aligned}$$

and, finally, $\mathtt{CP}^{\mathrm{L}}(\mathcal{L}_5) = \{(8,13,17),(6,7,19),(7,14,13),(10,21,8)\}$, as desired. Note that using either unidirectional approach requires the creation of a total of 36 labels, as opposed to the 25 required using coupling. □

Determining the best layer to couple on (i.e., the one in which the number of labels that need to be created is minimized) is a non-trivial. In particular, a unidirectional Pareto frontier compilation may require the creation of fewer labels than the bidirectional variant. We therefore propose the following heuristic procedure. Starting from $\mathbf{r}$ and $\mathbf{t}$, we first create $\mathcal{Z}^{\mathrm{TD}}(u')$ and $\mathcal{Z}^{\mathrm{BU}}(u'')$, respectively, for all $u' \in \mathcal{L}_2$ and for all $u'' \in \mathcal{L}_n$. Then, having constructed top-down labels for each node up to $\mathcal{L}_{j_1}$, $2 \le j_1$, and bottom-up labels for each node on or below $\mathcal{L}_{j_2}$, $j_2 \in [j_1+1, n]$, we pick among j_1 and j_2 the layer with the fewer number of total labels in order to proceed with the extension operations. Namely, if $\sum_{u \in \mathcal{L}_{j_1}} |\mathcal{Z}^{\mathrm{TD}}(u)| \le \sum_{u \in \mathcal{L}_{j_2}} |\mathcal{Z}^{\mathrm{BU}}(u)|$, extension of the top-down labels to $\mathcal{L}_{j_1+1}$ is completed and j_1 is set to j_1+1. Otherwise, extension of the bottom-up labels to $\mathcal{L}_{j_2-1}$ is completed, and j_2 is set to j_2-1. This procedure is repeated until $j_1 = j_2$, upon which coupling on layer $\mathcal{L}_{j_1}$ is used to calculate the Pareto frontier of the network model.

6.3 Label Removal Algorithms

Given a network model, the complexity of finding the Pareto frontier is largely determined by the cardinality of $\mathcal{Z}^{\mathrm{TD}}(u)$ and $\mathcal{Z}^{\mathrm{BU}}(u)$. Thus, having a VPO for the reduction of $|\mathcal{Z}^{\mathrm{TD}}(u)|$ and $|\mathcal{Z}^{\mathrm{BU}}(u)|$ is relevant for computational purposes.

The following proposition introduces such an operation. Given two nodes u, v in a same layer $\mathcal{L}_j$, the intuition behind the proposition is to identify when the subnetwork associated with $\mathcal{N}[u, \mathbf{t}]$ is dominated by $\mathcal{N}[v, \mathbf{t}]$, in which case we can remove labels in u that are dominated by v.

Proposition 3 (Label filtering). *Let u and v be two nodes in $\mathcal{L}_j$ for some $j \in [n]$. Suppose*

$$\mathtt{ND}\left(\mathtt{PF}\left(\mathcal{N}[u, \mathbf{t}]\right), \mathtt{PF}\left(\mathcal{N}[v, \mathbf{t}]\right)\right) = \mathtt{PF}\left(\mathcal{N}[v, \mathbf{t}]\right).$$

If there exists a pair of labels $\ell^u \in \mathcal{Z}^{\mathrm{TD}}(u)$ and $\ell^v \in \mathcal{Z}^{\mathrm{TD}}(v)$ for which $\ell^u \prec \ell^v$ (or $\ell^u = \ell^v$), then removing ℓ^u from $\mathcal{Z}^{\mathrm{TD}}(u)$ is a VPO. Similarly, if

$$\mathtt{ND}\left(\mathtt{PF}\left(\mathcal{N}[\mathbf{r}, u]\right), \mathtt{PF}\left(\mathcal{N}[\mathbf{r}, v]\right)\right) = \mathtt{PF}\left(\mathcal{N}[\mathbf{r}, v]\right),$$

and there exists $\ell^u \in \mathcal{Z}^{\mathrm{BU}}(u)$ and $\ell^v \in \mathcal{Z}^{\mathrm{BU}}(v)$ for which $\ell^u \prec \ell^v$ (or $\ell^u = \ell^v$), then removing ℓ^u from $\mathcal{Z}^{\mathrm{BU}}(u)$ is a VPO.

Proof. We provide a proof of the first case, as the proof of the other case follows by inverting the network model. By the condition in the statement of the proof, for each path p in $\mathcal{N}_{[u, \mathbf{t}]}$, it must be that $w(p) + \ell^u$ is dominated by $w(p') + \ell^v$, for some path p' in $\mathcal{N}_{[v, \mathbf{t}]}$. Thus $w(p) + \ell^u$ does not belong to $\mathtt{PF}(\mathcal{N})$ for any such p. It follows that the removal of ℓ^u is a VPO. □

Proposition 3 generalizes the concept of *state-based dominance* in DP (Bertsekas 2017) to network models. In particular, we can incorporate domain-specific information into a network model to identify cases where the conditions of Proposition 3 are satisfied. We provide an example instantiation in Section 7 which results in significant speedups in enumerating the Pareto frontier.

7 Numerical Study

In this section, we provide a detailed numerical evaluation of the effectiveness of the proposed algorithm on five different classes of problems. For each class, we discuss how the initial network

model is constructed, explain the best algorithmic configuration, and compare with existing state-of-the-art approaches for general MODOs. In particular, we consider the methodologies proposed by Kirlik and Sayın (2014) and Özlen et al. (2014), hereafter denoted by algorithms K and O, respectively. The source codes of these algorithms were kindly provided by the respective authors.

Experimental Design and Evaluation. All experiments ran on an Intel(R) Xeon(R) CPU E5-2680 v2 at 2.80GHz. Each experiment was limited to one thread and subject to a time limit of 3,600 seconds and a memory limit of 16GB. The algorithms K and O depend on the resolution of integer linear programs; we employed IBM ILOG CPLEX 12.7.1 with default settings for this task (IBM ILOG 2017). The paired Wilcoxon signed-rank test was used to estimate p-values comparing pairs of algorithms (Wilcoxon 1945) (this is a nonparametric test that will be used to compare if population mean ranks of solution times differ between algorithms).

Data was generated following previous literature guidelines; details of the random generation procedure for each problem class are presented in the appendix. Direct comparisons between the algorithms are presented in cumulative distribution plots, which show the number of instances solved by each algorithm (y-axis) within a given time limit (x-axis). We use the integral of the curve associated with an algorithm to estimate its relative performance so that the quality of an algorithm depends both on the running time and on the number of instances solved. The order in which algorithms are listed in the legends reflect this metric, with the best-performing algorithms appearing on the top. Additionally, we present scatter plots to compare the best-performing network model algorithm against the best previous state-of-the-art algorithm. These plots are presented in logarithmic scale and represent the amount of time the algorithms require to solve each instance of the given benchmark. We also employ a color code to indicate the size of the Pareto frontier of each instance.

The network model-based algorithms employing the bottom-up, top-down, and bidirectional Pareto frontier compilation are represented by BU, TD, and Coup, respectively. For applications where the domain-specific label filtering given in Proposition 3 has been applied, we denote the extensions of BU, TD, and Coup by BU+, TD+, and Coup+, respectively.

7.1 Multiobjective 0-1 Knapsack Problem

Given n items, a capacity $W > 0$, and for each item $i \in [n]$, a weight $w_i > 0$ and K profits $p_i^1, p_i^2, \ldots, p_i^K > 0$, the multiobjective 0-1 knapsack problem (MKP) is

$$\max \left\{ ((p^1)^\top x, (p^2)^\top x, \ldots, (p^K)^\top x) \, : \, w^\top x \leq W, \, x \in \mathbb{B}^n \right\}.$$

Network model construction. The initial network is constructed via a recursive formulation using a single dimensional state variable $s \in \mathbb{R}_+$, which corresponds to the total weight of the knapsack at a certain stage. The root state is $s_0 = 0$. We cannot set a variable $x_j = 1$ if it weighs more than the available capacity, i.e., $\mathcal{V}_j(s) := \{v \in \mathbb{B} : s + v \cdot w_j \leq W\}$. The transition functions update the total weight of the knapsack: $\tau_j(s, v) = s + v \cdot w_j$ for all $j \in [n-1]$ and $\tau_n(s, v) = W$. Lastly, for any $j \in [n]$, the reward function is the profit vector of item j, i.e., $\delta_j(s, v) := v \times \left(p_j^1, p_j^2, \ldots, p_j^K \right)$.

We incorporate the label filtering of Proposition 3 by exploiting the classical DP state dominance for knapsack problems. For any $j \in [n]$, let $u_i^j, u_{i'}^j \in \mathcal{L}_j$ be two possible states obtained at layer j using the aforementioned recursive model. If $u_i^j \geq u_{i'}^j$, we have

$$\texttt{ND} \left(\texttt{PF} \left(\mathcal{N}[u_i^j, \mathbf{t}] \right), \texttt{PF} \left(\mathcal{N}[u_{i'}^j, \mathbf{t}] \right) \right) = \texttt{PF} \left(\mathcal{N}[u_{i'}^j, \mathbf{t}] \right).$$

The equality above follows since each path (i.e., partial feasible solution) in $\mathcal{N}[u^j, \mathbf{t}]$ has a path in $\mathcal{N}[u^j_{i'}, \mathbf{t}]$ of same path-weight, given that we have more capacity available at $u^j_{i'}$ than u^j_i. That is, we can assign the same variable values in a path starting at $u^j_{i'}$ and incur the same objective function contribution. Thus, we can remove labels at u^j_i if they are dominated by a label at $u^j_{i'}$.

Computational evaluation. We experimented on 450 instances with $K \in \{3, 4, \ldots, 7\}$ objectives and $n \in \{20, 30, \ldots, 100\}$ variables. The detailed results are presented in Table 2 of the appendix. We provide an analysis of the results and summarize our findings.
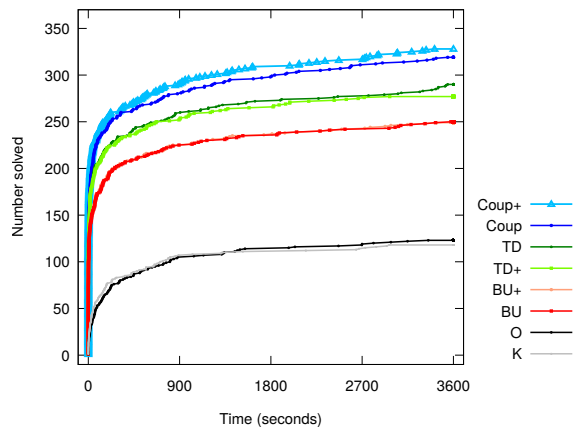

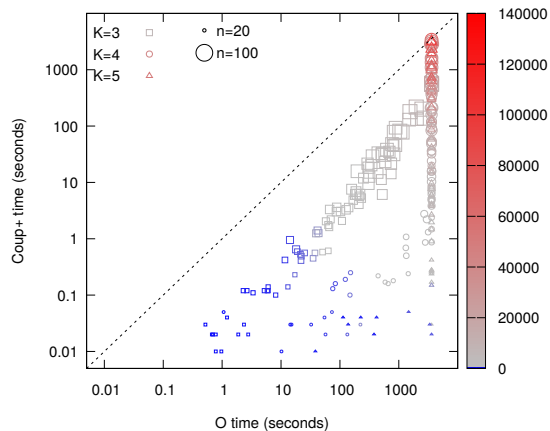**Figure 6:** Knapsack cumulative distribution plot

Figure 7: Knapsack scatter plot

The cumulative distribution plot for the knapsack instances is presented in Figure 6. The results show a clear dominance of all network model algorithms over O and K. Overall, Coup+ delivered the best results, solving 370 instances, whereas the configurations BU and BU+ were relatively weaker and solved 280 and 279 and instances, respectively. O and K solved 154 and 149, respectively. The figure also shows that the network model algorithms are considerably faster, as they solve more instances within seconds than O and K in one hour.

Figure 7 shows a scatter plot comparing Coup+ with O for instances with up to five objective functions. We removed from the plot instances with $K = 6$ and $K = 7$, since O and K have considerably worse performance and the results do not provide much insight. Coup+ was at least as efficient as O and K in every knapsack instance tested, and only three instances that could not be solved by this network model configuration were solved by the others (one by TD and two by Coup). The sizes of the Pareto frontier do not seem to affect the relative performance between Coup+ and O; namely, Coup+ and the other network model algorithms perform better than the previous state of the art in all cases, perhaps even more so in instances with smaller solution sets.

With respect to Pareto frontier compilation, the bidirectional strategy had the best results while bottom-up was relatively poor, independently from the inclusion of the label filtering VPO. Filtering affected network model algorithms in different ways, depending on the Pareto frontier compilation strategy used. The solution time differences between BU and BU+ are statistically significant (p-value of 10^{-9}), although in practical terms they perform similarly; the number of solved instances is almost the same (280 vs 279) and the average running time goes from 252 to 244 with filtering, a gain of 3% on average. The inclusion of filtering decreased the quality of the top-down algorithm, with 310 instances solved (as opposed to 323) and almost 40 seconds of additional computational time, on average, to solve instances solved by both algorithms (from 184 to 221, with p-value of 10^{-13}). Finally, Coup+ is significantly better than Coup (p-value of 10^{-40}); more instances were

solved (370 in comparison with 362) in less time (average running time reduced from 318 to 228) and less variability (standard deviation reduced from 710 to 525).

7.2 Multiobjective Set Covering and Set Partitioning Problems

We consider the multiobjective variants of the classical set covering and set partitioning problems. Namely, let $A \in \mathbb{B}^{m \times n}$ be a binary constraint coefficient matrix, and let $c^1, \ldots, c^K$ be K cost vectors in $\mathbb{R}^n$. The multiobjective set covering problem (MSCP) is defined as

$$\min \left\{ ((c^1)^\top x, (c^2)^\top x, \ldots, (c^K)^\top x) \, : \, Ax \geq \mathbf{1}, x \in \mathbb{B}^n \right\}.$$

The multiobjective set packing problem (MSPP) replaces "min" by "max" and the inequality sign from "$\geq$" to "$\leq$" in the definition above.

Network model construction.   The original networks are produced by employing the DD transformation discussed in Section 4.2. In particular, we used the set covering DD by Bergman et al. (2011) and the set packing DD by Bergman et al. (2014). In our experiments, label filtering for both applications did not impact performance, so we omit the corresponding results.

Computational evaluation.   We experimented on 150 random instances with $n \in \{100, 150, 200\}$. Detailed results for the MCSP and the MSPP are presented in Tables 3 and 4, respectively.

For the MSCP, `Coup` delivered the best results among the network model algorithms, solving 90 instances with an average running time of 81 seconds (and a standard deviation of 188). `TD` solved more instances (91), but its average runtime was higher (122 with a standard deviation of 263). Moreover, for the 88 instances solved by both, `Coup` had an average running time of 64 (with a standard deviation of 127), against 104 (standard deviation of 229) for `TD`.
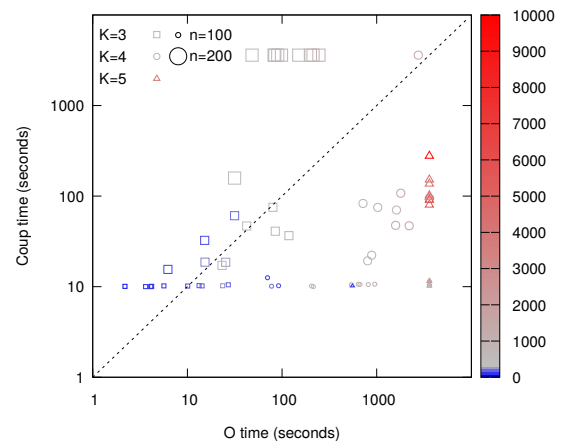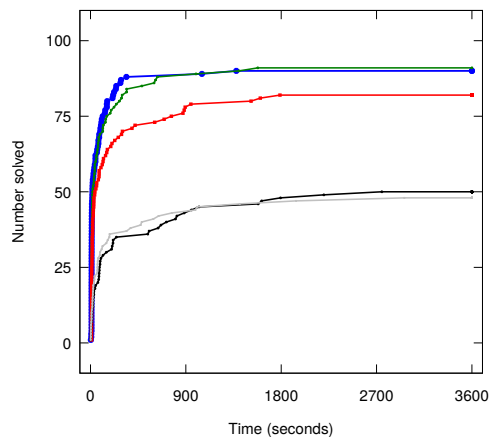
Figure 8: Set covering cumulative distribution plot

Figure 9: Set covering scatter plot

Algorithms `K` and `O` solved 48 and 50 instances, respectively. Among these, there were instances that the network model configurations could not enumerate the Pareto frontier (between 9 and 11, depending on the configuration employed). These instances were relatively large, typically of size $n = 200$, resulting in large network models that could not be solved within the given limits.

Figure 9 depicts the relative performance of `O` and `Coup` on the MSCP, in particular elucidating the one configuration for which `O` significantly outperformed `Coup` (200 variables, $K = 3$). However,

17

the same plot also suggests that `Coup` is far more efficient for instances with relatively large Pareto frontiers. This suggests that the performance of the network models are less sensitive to the size of the Pareto frontier than `K` and `O`.

The results for the MSPP are presented in the cumulative distribution plot in Figure 10 and in the scatter plot in Figure 11. `Coup` also delivered the best results for this problem class, slightly
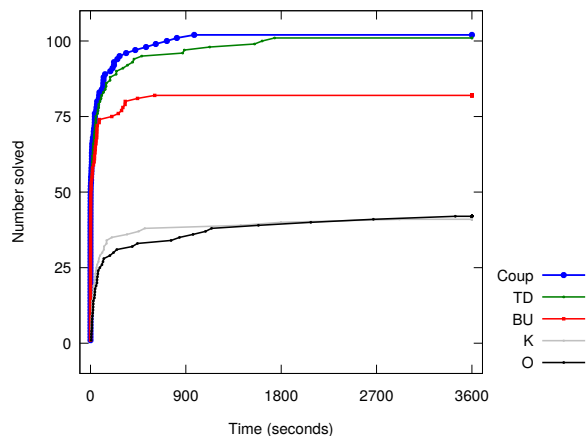
Figure 10: Set packing cumulative distribution plot
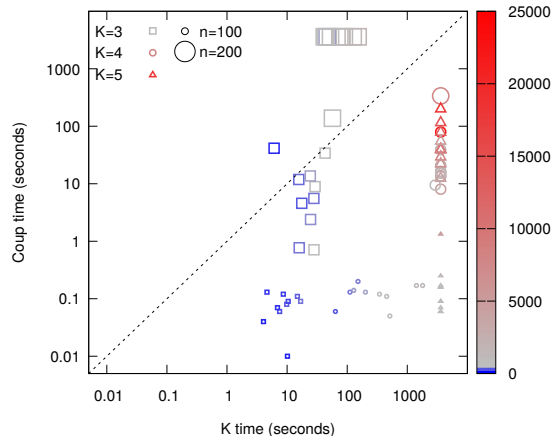
Figure 11: Set packing scatter plot

outperforming `TD`; `Coup` solved one more instances than `TD` (102 vs 101) and had smaller running times (averages of 71 versus 123 and standard deviation of 170 versus 322). `Coup` and `TD` solved more instances of the MSPP than the MSCP, whereas `BU`, `K`, and `O` had the inverse behavior. Algorithms `K` and `O` again solved fewer instances (41 and 42) and, among these, between 9 and 10 instances (depending on the configuration) were not solved by the network models. The size of the instances played a role in the efficiency of the algorithms. Figure 11 shows that `K` outperforms `Coup` in some instances, but in relatively fewer cases than in the MSCP. Moreover, the Pareto frontier sizes have the same impact on the relative performance of the algorithms, as in the case of the MSCP, showing the robustness of network models.

7.3 Multiobjective Traveling Salesperson Problem

The multiobjective traveling salesperson problem (MTSP) is a generalization of the classical TSP where arcs are associated with multiple (often conflicting) distance measures. That is, given a graph $G = (V, E)$ with vertex set $V = \{1, \ldots, n\}$ and where each edge $e \in E$ is associated with costs $c_e^1, \ldots, c_e^K$, MTSP asks for the nondominated Hamiltonian tours in G with respect to edge costs.

Network model construction. The initial network is constructed using the classical dynamic programming model for the TSP (Bertsekas 2017). Each state $s := (\bar{V}, v)$ is composed by a set $\bar{V} \subseteq V$, representing the vertices that are still left to be visited, and a vertex $v \in V \setminus \bar{V}$, representing the last visited vertex. The initial state is $s_0 := (V \setminus \{1\}, 1)$ (assuming we start and end at vertex 1). The variable x_j denotes the vertex that is visited at the j-th position of the Hamiltonian tour; thus, $\mathcal{V}_j((\bar{V}, v)) = x_j$. The transition function updates the set of visited vertices, $\tau_j((\bar{V}, v), x_j) = (\bar{V} \setminus \{x_j\}, x_j)$, and the reward function is the negative of the distance travelled (since we are maximizing), $\delta_j((\bar{V}, v), x_j) = (-c_{v, x_j}^1, \cdots, -c_{v, x_j}^K)$, for $j = 1, \ldots, n$. Finally,

we establish a special terminal state with $\delta_{n+1}((\emptyset, v), x_j) = (-c_{v,1}^1, \cdots, -c_{v,1}^K)$ that represents the return to vertex 1.

Computational evaluation. We experimented on 150 instances, with 10 instances for each configuration of $n \in \{5, 10, 15\}$ and $K \in \{3, 4, 5, 6, 7\}$. We only depict results by `Coup`, which dominated all other network-based configurations, and `K`, which also was superior to `O` in all scenarios tested. In particular, `K` uses the Miller-Tucker-Zemlin formulation of TSP (Miller et al. 1960) as in Özlen et al. (2014). Table 1 depicts the results, where column `P` gives the average size of the Pareto frontiers (taking into account only closed instances), `S` gives the number of problems solved for the associated technique, and $\bar{t}$ provides the average time (out of 10 instances with the configuration); small running times were rounded up to 1 second.

Table 1: Multiobjective Traveling Salesperson Problem Results

			Coup		K	
n	K	P	S	$\bar{t}$	S	$\bar{t}$
5	3	6.9	10	1.0	10	1.0
	4	8.7	10	1.0	10	1.0
	5	8.1	10	1.0	10	1.2
	6	11.0	10	1.0	10	2.8
	7	10.9	10	1.0	5	11.4
10	3	163.1	10	1.0	10	57.1
	4	675.7	10	1.0	7	2021.4
	5	2040.2	10	1.0	0	-
	6	20080.5	10	1.0	0	-
	7	9716.7	10	1.9	0	-
15	3	670.7	10	3.2	7	2338.9
	4	8328.5	10	41.2	0	-
	5	55875.0	10	543.9	0	-
	6	190447.3	8	2462.1	0	-
	7	-	0	-	0	-

Our results show a complete dominance of `Coup` over `K`. Namely, `Coup` was superior to `K` by at least one order of magnitude in all instances; for some configurations, `K` could not solve a single instance, whereas `Coup` closed all scenarios within seconds (see e.g., $n = 10$ and $K = 7$). Instances with 15 cities are very challenging for current state-of-the-art techniques; note that neither `K` nor `Coup` managed to solve any instance with $n = 15$ and $K = 7$; observe also that the size of the Pareto frontiers increase significantly with n and K. Nevertheless, `Coup` shows significant superiority in these scenarios as well; whereas `K` could not close any instances where $K \geq 4$, `Coup` solved all instances with up to 5 objective functions in less than 10 minutes in average, and 8 out of 10 instances with $K = 6$.

7.4 Multiobjective Cardinality-Constrained Absolute Value Problem

The multiobjective cardinality-constrained absolute value problem (MCCAVP) is defined as

$$\min \left\{ \left(\left| (a^1)^\top x - b_1 \right|, \left| (a^2)^\top x - b_2 \right|, \ldots, \left| (a^K)^\top x - b_K \right| \right) : \mathbf{1}^\top x \leq C, x \in \mathbb{B}^n \right\},$$

where $a^1, \ldots, a^K \in \mathbb{Z}^n, b \in \mathbb{Z}^K$, and $C \in \mathbb{Z}_+$. The MCCAVP is a multiobjective variant of the discrete L_1-norm minimization problems, classically applied in statistical data fitting and circuit optimization (Jong 2012, Narula and Wellington 1982). For instance, in data fitting problems each linear function represents a residual, and in the multiobjective case we wish to evaluate the Pareto frontier of nondominated fitting configurations according to each residual.

The MCCAVP illustrates how the procedure generalizes to multiobjective nonlinear applications. If any of the K objective functions is instead written as a linear function raised to the power of $\alpha \in \mathbb{Z}_{\geq 1}$, the outer function can be replaced by the absolute value (if α is even) or simply ignored (if α is odd) without affecting the Pareto frontier. The MCCAVP therefore provides a modeling framework for a wide-range of objective functions.

Network model construction. The initial network is constructed via a multiobjective recursive formulation as presented in Section 4.1. The recursive formulation is obtained by using a $(K+1)$-dimensional state variable $s := (\theta, \gamma) \in \mathbb{R}^K \times \mathbb{R}$, where $\theta_1, \ldots, \theta_K$ represent the partial evaluation of each $(a^k)^\top x$ for all $k \in [K]$, and γ is the number of variables that are set to one at that stage. The root state is $s_0 = (b, 0)$. We cannot set a variable $x_j = 1$ if it exceeds the available capacity, i.e., $\mathcal{V}_j(s) := \{v \in \mathbb{B} : \gamma + v \leq C\}$. The transition functions update the partial evaluation of $(a^k)^\top x$ and the number of variables that are set to one; i.e.,

$$\tau_j(s, v) = (\theta_1 + a_j^1 \cdot v, \theta_2 + a_j^2 \cdot v, \ldots, \theta_K + a_j^K \cdot v, \gamma + v).$$

for all $j \in [n]$. The reward function is the change in each objective function when transitioning from state $s = (\theta, \gamma)$ to another, that is, the k-th component of $\delta_j(s, v)$ is given by

$$\left(\delta_j(s, v) \right)_k := |\theta_k + a_j^k \cdot v - b_k| - |\theta_k - b_k|,$$

for $k \in [k]$. To verify its validity, fix $k \in [K]$ and consider any feasible $x = (v_1, \ldots, v_n)$ and the associated state transitions $s_0 = (\theta^0, \gamma^0), s_1 = (\theta^1, \gamma^1), \ldots, s_n = (\theta^n, \gamma^n)$. Observe that, by definition,

$$\sum_{j=1}^n \left(\delta_j(s_{j-1}, v_j) \right)_k = |\underbrace{\theta_k^0 + a_1^k \cdot v_1}_{\theta_k^1} - b_k| - |\theta_k^0 - b_k| + |\underbrace{\theta_k^1 + a_2^k \cdot v_2}_{\theta_k^2} - b_k| - |\theta_k^1 - b_k|$$

$$+ |\underbrace{\theta_k^2 + a_3^k \cdot v_3}_{\theta_k^3} - b_k| - |\theta_k^2 - b_k| + \cdots + |\underbrace{\theta_k^{n-1} + a_n^k \cdot v_n}_{\theta_k^n} - b_k| - |\theta_k^{n-1} - b_k|$$

$$= |\theta_k^n - b_k| - \underbrace{|\theta_k^0 - b_k|}_{0} = \left| \sum_{j=1}^n a_j^k v_j - b_k \right|,$$

which is the original objective for the k-th function.

Mixed-Integer Linear Programming Reformulation. Since the original formulation for the MCCAVP is nonlinear, it cannot be directly input to K and O. We consider the following linear reformulation of the MCCAVP for K and O:

$$\min_{x \in \mathbb{B}^n, \mathbf{1}^\top x \leq C} \{y_1, \ldots, y_K\}$$

$$\text{s.t. } y_k \geq (a^k)^\top x - b_k, \qquad k \in [K],$$

$$y_k \geq -(a^k)^\top x + b_k, \qquad k \in [K].$$

Computational evaluation. We experimented on 6,250 random instances. The detailed results for the MCCAVP are presented in Table 5. In particular, all cases were solved by each network-based configuration. For this section, we restrict the analysis of the results to 450 of these instances, which have $M = 250$, $n \geq 15$, and $C \geq 30$, as the others were solved within a few seconds.

The cumulative distribution plot is presented in Figure 12. Whereas K and O solved less than 200 instances each, the network algorithms enumerated the Pareto frontier in less than 10 minutes in each case. Over the complete benchmark set, BU delivered the best results. For the restricted set of 450 instances, BU was also the best, although its results (average running time of 18 seconds with standard deviation of 41) were not different from those obtained by TD (average of 24 and standard deviation of 69) in a statistically significant way (p-value of 0.026).

Algorithm O solved more instances than K in the extended dataset (4,118 vs. 4,108), albeit with a higher runtime (on average 30% larger). Alternatively, for the restricted family of instances, K solved more instances (178 vs. 172) with a much shorter runtime (average of 258 and standard deviation of 492 vs. average of 432 and standard deviation of 801), thus suggesting that K outperforms O for harder instances. We therefore select K for further comparison.
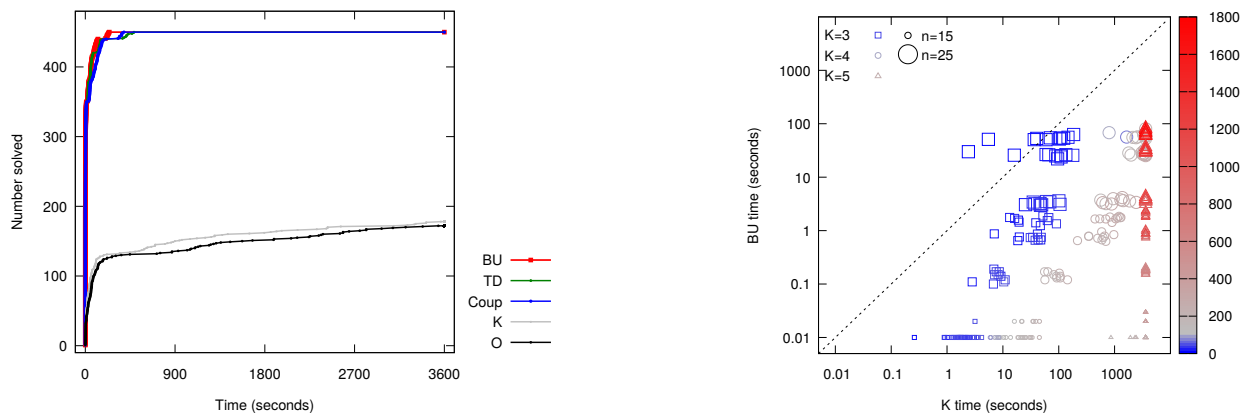
Figure 12: Absolute value cumulative distribution plot **Figure 13:** Absolute value scatter plot

Figure 13 shows a scatter plot comparing the performance of BU with K. Algorithm K outperforms BU in 5 instances by one order of magnitude (2 vs 30 seconds was the largest relative difference). All instances solved by K were also successfully addressed by BU, with an average running time of 8 seconds and standard deviation of 17. Furthermore, similar to what was observed for the MSCP and MSPP, there is a positive correlation between the size of the Pareto frontiers and the relative superiority of network model procedures over K and O.

8 Conclusion

This paper presents a novel framework for solving multiobjective discrete optimization problems (MODOs) through a reformulation into *network models*, enhanced by validity-preserving operations that reduce the size of the network while preserving the Pareto frontier. The generality of the framework is established through application to five distinct problem classes, including a nonlinear multiobjective optimization problem. The experimental evaluation suggests that the proposed algorithm outperforms exisiting state-of-the-art general MODO solvers in several multiobjective variants of classical operations research problems.

Our methodology assumes memory availability exceeds memory requirements for constructing

and storing network models. Since multiobjective optimization problems become rapidly more challenging as problem size grows, this was only a limiting factor for the largest of instances generated, most of which were beyond the scope of other algorithms we tested against. As memory availability in modern-day CPUs continues to grow, investigating algorithms specifically designed to exploit this resource is of great interest, and this paper provides an aimed step in this direction.

References

N. Adelgren and A. Gupte. Branch-and-bound for biobjective mixed integer programming, 2017. https://arxiv.org/pdf/1709.03668.pdf.

C. Bazgan, H. Hugot, and D. Vanderpooten. Solving efficiently the 0-1 multi-objective knapsack problem. *Comput. and Oper. Res.*, 36(1):260–279, 2009.

Markus Behle. On threshold bdds and the optimal variable ordering problem. *Journal of Combinatorial Optimization*, 16(2):107–118, 2007.

T. Bektas. Disjunctive programming for multiobjective discrete optimisation, 2016. http://www.optimization-online.org/DB_FILE/2016/05/5442.pdf.

D. Bergman, W.-J. van Hoeve, and J.N. Hooker. Manipulating MDD Relaxations for Combinatorial Optimization. In Tobias Achterberg and J. Beck, editors, *Integration of AI and OR Techniques in Constraint Programming for Combinatorial Optimization Problems*, volume 6697 of *Lecture Notes in Computer Science*, chapter 5, pages 20–35. Springer Berlin / Heidelberg, Berlin, Heidelberg, 2011.

D. Bergman, A. A. Cire, W.-J. Jan van Hoeve, and T. H. Yunes. BDD-based heuristics for binary optimization. *Journal of Heuristics*, 20(2):211–234, 2014.

D. Bergman, A.A. Cire, W.J. van Hoeve, and J. Hooker. *Decision diagrams for optimization*. Springer, 2016.

David Bergman and Andre A. Cire. Multiobjective optimization by decision diagrams. In Michel Rueher, editor, *Principles and Practice of Constraint Programming: 22nd International Conference, CP 2016, Toulouse, France, September 5-9, 2016, Proceedings*, pages 86–95. Springer International Publishing, Cham, 2016.

Dimitri P. Bertsekas. *Dynamic Programming and Optimal Control*, volume 1. Athena Scientific, 4th edition, 2017.

Dimitris Bertsimas and John N Tsitsiklis. *Introduction to Linear Optimization*, volume 6. Athena Scientific, 1997.

G.R. Bitran. Linear multiple objective programs with zero-one variables. *Math. Program.*, 13(1):121–139, 1977.

G.R. Bitran and J.M. Rivera. A combined approach to solve binary multicriteria problems. *Naval Res. Logist.*, 29(2):181–201, 1982.

M. Bodur, S. Ahmed, N. Boland, and G.L. Nemhauser. Decomposition of loosely coupled integer programs: A multiobjective perspective, 2016. http://www.optimization-online.org/DB_FILE/2016/08/5599.pdf.

N. Boland, H. Charkhgard, and M. Savelsbergh. A criterion space search algorithm for biobjective integer programming: The balanced box method. *INFORMS J. Comput.*, 27(4):735–754, 2015.

N. Boland, H. Charkhgard, and M. Savelsbergh. The L-shape search method for triobjective integer programming. *Math. Program. Comput.*, 8(2):217–251, 2016a.

N. Boland, H. Charkhgard, and M. Savelsbergh. A new method for optimizing a linear function over the efficient set of a multiobjective integer program. *European J. Oper. Res.*, 2016b.

N. Boland, H. Charkhgard, and M. Savelsbergh. The quadrant shrinking method: A simple and efficient algorithm for solving tri-objective integer programs. *European J. Oper. Res.*, 2016c.

S. Borzsony, D. Kossmann, and K. Stocker. The skyline operator. In *Data Engineering, 2001. Proceedings. 17th International Conference on*, pages 421–430. IEEE, 2001.

Christiane Regina Soares Brasil, Alexandre Claudio Botazzo Delbem, and Fernando Lus Barroso da Silva. Multiobjective evolutionary algorithm with many tables for purely ab initio protein structure prediction. *Journal of Computational Chemistry*, 34(20):1719–1734, 2013.

R. E. Bryant. Graph-based algorithms for boolean function manipulation. *IEEE Transactions on Computers*, C-35:677–691, 1986.

R. E. Bryant. Symbolic boolean manipulation with ordered binary decision diagrams. *ACM Computing Surveys*, 24:293– 318, 1992.

M.E. Captivo, J. Clımaco, J. Figueira, E. Martins, and J.L. Santos. Solving bicriteria 0-1 knapsack problems using a labeling algorithm. *Comput. and Oper. Res.*, 30(12):1865–1886, 2003.

R.L. Carraway, T.L. Morin, and H. Moskowitz. Generalized dynamic programming for multicriteria optimization. *European J. Oper. Res.*, 44(1):95–104, 1990.

K. Dächert and K. Klamroth. A linear bound on the number of scalarizations needed to solve discrete tricriteria optimization problems. *J. Global. Opt.*, pages 1–34, 2015.

C. Delort and O. Spanjaard. Using bound sets in multiobjective optimization: Application to the biobjective binary knapsack problem. *Lecture Notes in Computer Science*, 6049:253–265, 2010.

Clarisse Dhaenens, Julien Lemesre, and El-Ghazali Talbi. *k*-ppm: A new exact method to solve multi-objective combinatorial optimization problems. *European J. Oper. Res.*, 200(1):45–53, 2010.

Jörg Thomas Dickersbach. *Supply Chain Management with APO: Structures, Modelling Approaches and Implementation of MySAP SCM 4.1.* Springer, Berlin, 2 edition, 2015.

João A. Duro and Dhish Kumar Saxena. Timing the decision support for real-world many-objective optimization problems. In Heike Trautmann, Günter Rudolph, Kathrin Klamroth, Oliver Schütze, Margaret Wiecek, Yaochu Jin, and Christian Grimme, editors, *Evolutionary Multi-Criterion Optimization*, pages 191–205. Springer International Publishing, 2017. ISBN 978-3-319-54157-0.

M. Ehrgott. A discussion of scalarization techniques for multiple objective integer programming. *Ann. Oper. Res.*, 147(1):343–360, 2006a.

M. Ehrgott. *Multicriteria optimization.* Springer Science & Business Media, 2006b.

M. Ehrgott, X. Gandibleux, and A. Przybylski. Exact methods for multi-objective combinatorial optimisation. In *Multiple Criteria Decision Analysis*, pages 817–850. Springer, 2nd edition, 2016.

J.R. Figueira, G. Tavares, and M.M. Wiecek. Labeling algorithms for multiple objective integer knapsack problems. *Comput. and Oper. Res.*, 37(4):700–711, 2010.

J.R. Figueira, L. Paquete, M. Simões, and D. Vanderpooten. Algorithmic improvements on dynamic programming for the bi-objective {0, 1} knapsack problem. *Comp. Opt. and Appl.*, 56(1):97–111, 2013.

Lucie Galand, Anisse Ismaili, Patrice Perny, and Olivier Spanjaard. Bidirectional preference-based search for state space graph problems. In *Proceedings of the Sixth Annual Symposium on Combinatorial Search, SOCS 2013, Leavenworth, Washington, USA, July 11-13, 2013.*, 2013.

R. G. Garroppo, S. Giordano, and L. Tavanti. A survey on multi-constrained optimal path computation: Exact and approximate algorithms. *Computer Networks*, 54(17):3081 – 3107, 2010.

Jonathan M. Gomes-Selman, Qinru Shi, Yexiang Xue, Roosevelt García-Villacorta, Alexander S. Flecker, and Carla P. Gomes. Boosting efficiency for computing the pareto frontier on tree structured networks. In Willem-Jan van Hoeve, editor, *Integration of Constraint Programming, Artificial Intelligence, and Operations Research*, pages 263–279. Springer International Publishing, 2018. ISBN 978-3-319-93031-2.

Satyaveer Goud Gudala. Skyline queries for multi-criteria decision support systems. Master's thesis, Kansas State University, 2012.

T. Hadzic and J. N. Hooker. Cost-bounded binary decision diagrams for 0-1 programming. In E. Loute and L. Wolsey, editors, *Proceedings of the International Workshop on Integration of Artificial Intelligence and Operations Research Techniques in Constraint Programming for Combinatorial Optimization Problems (CPAIOR 2007)*, volume 4510 of *Lecture Notes in Computer Science*, pages 84–98. Springer, 2007.

Y.Y. Haimes, L.S. Lasdon, and D.A. Wismer. On a bicriterion formulation of the problems of integrated system identification and system optimization. *IEEE Trans. Syst. Man and Cybern.*, 1(1):296–297, 1971.

M. I. Henig. The shortest path problem with two objective functions. *European Journal of Operational Research*, 25(2):281 – 291, 1986.

John N. Hooker. Decision diagrams and dynamic programming. In Carla Gomes and Meinolf Sellmann, editors, *Integration of AI and OR Techniques in Constraint Programming for Combinatorial Optimization Problems: 10th International Conference, CPAIOR 2013, Yorktown Heights, NY, USA, May 18-22, 2013. Proceedings*, pages 94–110. Springer Berlin Heidelberg, Berlin, Heidelberg, 2013.

IBM ILOG. CPLEX Optimization Studio 12.7.1 user manual, 2017.

Yunchol Jong. An augmented smoothing method of l1 -norm minimization and its implementation by neural network model, 2012. https://arxiv.org/abs/1207.1931.

N. Jozefowiez, G. Laporte, and F. Semet. A generic branch-and-cut algorithm for multiobjective optimization problems: Application to the multilabel traveling salesman problem. *INFORMS J. Comput.*, 24(4): 554–564, 2012.

G. Kirlik and S. Sayın. A new algorithm for generating all nondominated solutions of multiobjective discrete optimization problems. *European J. Oper. Res.*, 232(3):479–488, 2014.

K. Klamroth and M.M. Wiecek. Dynamic programming approaches to the multiple criteria knapsack problem. *Naval Res. Logist.*, 47(1):57–76, 2000.

D. Klein and E. Hannan. An algorithm for the multiple objective integer linear programming problem. *European J. Oper. Res.*, 9(4):378–385, 1982.

M. Laumanns, L. Thiele, and E. Zitzler. An adaptive scheme to generate the pareto front based on the epsilon-constraint method. In *Dagstuhl Seminar Proceedings*. Schloss Dagstuhl-Leibniz-Zentrum für Informatik, 2005.

M. Laumanns, L. Thiele, and E. Zitzler. An efficient, adaptive parameter variation scheme for metaheuristics based on the epsilon-constraint method. *European J. Oper. Res.*, 169(3):932–942, 2006.

B. Lokman and M. Köksalan. Finding all nondominated points of multi-objective integer programs. *J. Global. Opt.*, 57(2):347–365, 2013.

M. Masin and Y. Bukchin. Diversity maximization approach for multiobjective optimization. *Oper. Res.*, 56 (2):411–424, 2008.

G. Mavrotas and D. Diakoulaki. A branch and bound algorithm for mixed zero-one multiple objective linear programming. *European J. Oper. Res.*, 107(3):530–541, 1998.

G. Mavrotas and D. Diakoulaki. Multi-criteria branch and bound: A vector maximization algorithm for mixed 0-1 multiple objective linear programming. *Appl. Math. Comput.*, 171(1):53–71, 2005.

C.E. Miller, A.W. Tucker, and R.A. Zemlin. Integer programming formulation of traveling salesman problems. *Journal of the ACM (JACM)*, 7(4):326–329, 1960.

Subhash C. Narula and John F. Wellington. The minimum sum of absolute errors regression: A state of the art survey. *International Statistical Review / Revue Internationale de Statistique*, 50(3):317–326, 1982.

M. Özlen and M. Azizoğlu. Multi-objective integer programming: a general approach for generating all non-dominated solutions. *European J. Oper. Res.*, 199(1):25–35, 2009.

M. Özlen, B.A. Burton, and C.A.G. MacRae. Multi-objective integer programming: An improved recursive algorithm. *J. Optim. Theory Appl.*, 160(2):470–482, 2014.

Ö. Özpeynirci and M. Köksalan. An exact algorithm for finding extreme supported nondominated points of multiobjective mixed integer programs. *Management Sci.*, 56(12):2302–2315, 2010.

S.N. Parragh and F. Tricoire. Branch-and-bound for bi-objective integer programming, 2015. http://www.optimization-online.org/DB_FILE/2014/07/4444.pdf.

A. Przybylski, X. Gandibleux, and M. Ehrgott. A two phase method for multi-objective integer programming and its application to the assignment problem with three objectives. *Discrete Optim.*, 7(3):149–165, 2010.

T.K. Ralphs, M.J. Saltzman, and M.M. Wiecek. An improved algorithm for solving biobjective integer programs. *Ann. Oper. Res.*, 147(1):43–70, 2006.

A. Rong and J.R. Figueira. A reduction dynamic programming algorithm for the bi-objective integer knapsack problem. *European J. Oper. Res.*, 231(2):299–313, 2013.

A. Rong and J.R. Figueira. Dynamic programming algorithms for the bi-objective integer knapsack problem. *European J. Oper. Res.*, 236(1):85–99, 2014.

A. Rong, J.R. Figueira, and M.V. Pato. A two state reduction based dynamic programming algorithm for the bi-objective 0–1 knapsack problem. *Comp. & Math. with Appl.*, 62(8):2913–2930, 2011.

S. Sayın and P. Kouvelis. The multiobjective discrete optimization problem: A weighted min-max two-stage optimization approach and a bicriteria algorithm. *Management Sci.*, 51(10):1572–1581, 2005.

F. Sourd and O. Spanjaard. A multiobjective branch-and-bound framework: Application to the biobjective spanning tree problem. *INFORMS J. Comput.*, 20(3):471484, 2008.

R.E. Steuer and E.U. Choo. An interactive weighted tchebycheff procedure for multiple objective programming. *Math. Program.*, 26(3):326–344, 1983.

T. Stewart, O. Bandte, H. Braun, N. Chakraborti, M. Ehrgott, M. Göbelt, Y. Jin, H. Nakayama, S. Poles, and D. Di Stefano. Real-world applications of multiobjective optimization. *Multiobjective Optimization*, pages 285–327, 2008.

Thomas Stidsen, Kim Allan Andersen, and Bernd Dammann. A branch and bound algorithm for a class of biobjective mixed integer programs. *Management Science*, 60(4):1009–1032, 2014.

J. Sylva and A. Crema. A method for finding the set of non-dominated vectors for multiple objective integer linear programs. *European J. Oper. Res.*, 158(1):46–55, 2004.

Zbigniew Tarapata. Selected multicriteria shortest path problems: an analysis of complexity, models and adaptation of standard algorithms. *International Journal of Applied Mathematics and Computer Science*, 17(2):269287, 2007.

D. Tenfelde-Podehl. A recursive algorithm for multiobjective combinatorial optimization problems with Q criteria. Technical report, Institut für Mathematik, Technische Universität Graz, 2003.

B. Villarreal and M.H. Karwan. Multicriteria integer programming: A (hybrid) dynamic programming recursive approach. *Math. Program.*, 21(1):204–223, 1981.

B. Villarreal and M.H. Karwan. Multicriteria dynamic programming with an application to the integer case. *J. Optim. Theory Appl.*, 38(1):43–69, 1982.

T. Vincent, F Seipp, S Ruzika, A Przybylski, and X Gandibleux. Multiple objective branch and bound for mixed 0-1 linear programming: Corrections and improvements for biobjective case. *Comput. and Oper. Res.*, 40(1):498–509, 2013.

Wei Wang, Rong Mo, and Yan Zhang. Multi-objective aerodynamic optimization design method of compressor rotor based on isight. *Procedia Engineering*, 15(Supplement C):3699 – 3703, 2011.

Frank Wilcoxon. Individual comparisons by ranking methods. *Biometrics bulletin*, 1(6):80–83, 1945.

Yan Yu, J.B Zhang, Gang Cheng, M.C Schell, and Paul Okunieff. Multi-objective optimization in radiotherapy: applications to stereotactic radiosurgery and prostate brachytherapy. *Artificial Intelligence in Medicine*, 19(1):39 – 51, 2000. Evolutionary Computation in Medicine.

A. Zhou, B.-Y. Qu, H. Li, S.-Z. Zhao, P. N. Suganthan, and Q. Zhang. Multiobjective evolutionary algorithms: A survey of the state of the art. *Swarm and Evol. Comput.*, 1(1):32 – 49, 2011.

A Proofs

In this section we present the proofs for the structural results presented in the main text.

A.1 Proof of Theorem 1

Let $\mathcal{N}'$ be the network model that results from the application of the three operations stated in Theorem 1 on nodes u_1, u_2 of $\mathcal{N}$. We claim that there exists a one-to-one mapping between path-weights in $\mathcal{P}_\mathcal{N}$ and path-weights in $\mathcal{P}_{\mathcal{N}'}$; i.e., for each path in $\mathcal{P}_\mathcal{N}$, there is a path in $\mathcal{P}_{\mathcal{N}'}$ with same path-weight and vice-versa.

First, every path $p \in \mathcal{P}_\mathcal{N}$ that does not cross u_2 remains unchanged in $\mathcal{P}_{\mathcal{N}'}$, thus the equivalence follows in this case. Let us assume now that $p = (a_1, \ldots, a_i, a_{i+1}, \ldots, a_n)$ is a path in $\mathcal{P}_\mathcal{N}$ such that $t(a_i) = r(a_{i+1}) = u_2$. After the sequence of operations specified in the statement of the theorem, arc a_i is substituted for an arc a_i' in $\mathcal{N}'$ such that $r(a_i') = r(a_i)$, $t(a_i') = u_1$, and $w(a_i') = w(a_i)$, whereas arc a_{i+1} is substituted for an arc a_{i+1}' in $\mathcal{N}'$ such that $r(a_{i+1}') = u_1$, $t(a_{i+1}') = t(a_{i+1})$, and $w(a_{i+1}') = w(a_{i+1})$. These operations yield a one-to-one relationship between p and the path $p' = (a_1, \ldots, a_i', a_{i+1}', \ldots, a_n)$ in $\mathcal{N}'$ which, by construction, is such that $w(p') = w(p)$. Finally, as no additional paths are introduced, each path in $\mathcal{P}_{\mathcal{N}'}$ is also a path in $\mathcal{P}_\mathcal{N}$, so the result follows. □

A.2 Proof of Proposition 2

Weight-shift and node-merge operations can be implemented in a *bottom-up* iterative procedure as follows. Starting from the penultimate layer, we construct the vector $\tilde{c}(u)$ for each node $u \in \mathcal{L}_n$ by taking the componentwise minimum arc-weight among arcs in $\mathcal{A}^+(u)$. Once $\tilde{c}(u)$ has been obtained, the arc-weights can then be shifted up according to the VPO described in Proposition 1. Each arc is inspected twice (for the identification of the minimum first and for the shift operation afterwards) and each node is visited once; thus, this operation can be performed over the complete network in time $\mathcal{O}(K(|\mathcal{L}| + |\mathcal{A}|))$.

Checking whether nodes u_1, u_2 in layer $\mathcal{L}_i$ satisfy the merging conditions of Theorem 1 is an operation that can be performed in time $\mathcal{O}(K|\mathcal{L}_{i+1}|)$ if an adequate data structure is employed. Let π be an (arbitrary) ordering associated with the nodes of layer $\mathcal{L}_{i+1}$ and let π_j denote the j-th node of $\mathcal{L}_{i+1}$ according to this ordering, with the first position starting from zero. Given π, one can construct a $K|\mathcal{L}_{i+1}|$-dimensional vector $\xi(u)$ associated with each node u of layer $\mathcal{L}_i$ such that $(\xi(u))_{Kj+k} = w((u, \pi_j))_k$, i.e., entry $Kj + k$ contains the value of the k-th coordinate of the arc-weight associated with the arc connecting u to vertex π_j in $\mathcal{L}_{i+1}$; some arbitrary value, such as $-\infty$, may be employed for entries associated with absent arcs. If the verification above is performed for each pair of nodes composing layer $\mathcal{L}_i$, all merging operations can be verified in time $\mathcal{O}(K|\mathcal{L}_i|^2|\mathcal{L}_{i+1}|)$. As each pair of nodes in the network is compared at most once, we have a total running time of $\mathcal{O}(K|\mathcal{L}|^3)$.

□

A.3 Proof of Theorem 2

We consider a reduction from the following NP-Hard problem, written in terms of our notation and objective sense:

UNCONSTRAINED BIOBJECTIVE (Ehrgott 2006b, Proposition 8.12): Given $c^1, c^2 \in \mathbb{Z}^n$ and $d_1, d_2 \in \mathbb{Z}$, does there exist $x \in \mathbb{B}^n$ such that $\sum_{j=1}^n c_j^1 x_j \geq d_1$ and $\sum_{j=1}^n c_j^2 x_j \geq d_2$?

Let c^1, c^2, and $d := (d_1, d_2)$ define the parameters of an instance of the unconstrained biobjective problem. Equivalently, the problem asks if the given vector d is dominated by a point in the image space of the MODO defined as

$$\max \left\{ (c^1)^\top x, (c^2)^\top x : x \in \mathbb{B}^n \right\}. \tag{UCB}$$

We construct a network $\tilde{\mathcal{N}}$ where deciding if $d \in \mathcal{Y}_{\mathrm{N}}(\tilde{\mathcal{N}})$ is equivalent to applying an arc-removal VPO for an appropriate subset of the arcs of $\tilde{\mathcal{N}}$. To this end, let us first consider a valid network model $\mathcal{N} = (\mathcal{L}, \mathcal{A})$ for UCB. Since there are no constraints, we can construct a straightforward valid network model with one node per layer $\mathcal{L}_j$, $j \in [n+1]$, and two arcs a_1, a_2 connecting the node u_1 from layer $\mathcal{L}_j$ to node u_2 in layer $\mathcal{L}_{j+1}$, $j \in [n]$. In particular, $w(a_1) = \mathbf{0}$ (representing the assignment $x_j = 0$) and $w(a_2) = \left(c_j^1, c_j^2\right)$ (representing the assignment $x_j = 1$). The network $\mathcal{N}$ is depicted in Figure 14(a). Note that it has size polynomial in n, consisting of $n + 1$ nodes and $2n$ arcs.

(a) $\mathcal{N}$ (b) $\mathcal{N}'$
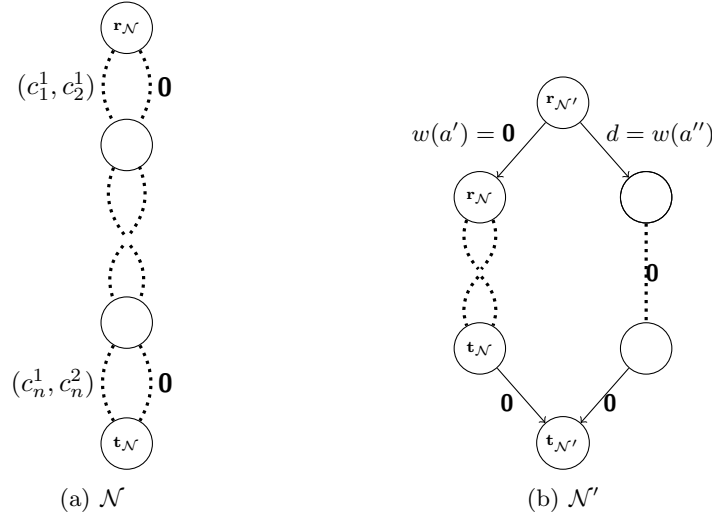
Figure 14: A network model $\mathcal{N}$ of a binary unconstrained MODO (a), and an extended network model $\tilde{\mathcal{N}}$ of $\mathcal{N}$ (b), used in the proof of Theorem 2.

We now design a new network model $\tilde{\mathcal{N}}$ by extending $\mathcal{N}$ as depicted in Figure 14(b). The root node $\mathbf{r}_{\tilde{\mathcal{N}}}$ is the arc-root of two arcs a' and a''. Arc a' has arc-weight $w(a') = \mathbf{0}$ and connects $\mathbf{r}_{\tilde{\mathcal{N}}}$ to the corresponding $\mathbf{r}_{\mathcal{N}}$ in the new network. Arc a'' has arc-weight $w(a'') = d$, and $\tilde{\mathcal{N}}$ contains a single path $p'' = (\mathbf{r}_{\tilde{\mathcal{N}}}, t(a''), \dots, \mathbf{t}_{\tilde{\mathcal{N}}})$ connecting $\mathbf{r}_{\tilde{\mathcal{N}}}$ to $\mathbf{t}_{\tilde{\mathcal{N}}}$ that traverses node $t(a'')$; the arc-weight of all arcs in p'' (except a'') is equal to zero. Finally, a single arc with arc-weight $\mathbf{0}$ connects $\mathbf{t}_{\tilde{\mathcal{N}}}$ to the associated $\mathbf{t}_{\mathcal{N}}$ in the new node.

Let $\mathcal{A}'$ be the subset of $\mathcal{A}_{\tilde{\mathcal{N}}}$ containing all arcs that compose path p''. If d is dominated by $\mathcal{Y}_{\mathrm{N}}(\tilde{\mathcal{N}})$, any arc a in $\mathcal{A}'$ may be removed from $\tilde{\mathcal{N}}$ without changing its Pareto frontier, i.e., $\mathrm{PF}\left(\tilde{\mathcal{N}}\right) = \mathrm{PF}\left(\tilde{\mathcal{N}} - a\right)$. Otherwise, by construction, d necessarily belongs to $\mathrm{PF}\left(\tilde{\mathcal{N}}\right)$, thus $d \in \mathrm{PF}(\mathcal{N})$. Hence, no arc is removed from $\mathcal{A}'$. Since all steps are polynomially bounded on n, the result follows. $\qquad\square$

A.4   Proof of Theorem 3

Suppose by contradiction that there exists a pair of nodes u and v that are isolating in $\mathcal{N}$, together with an arc a whose removal is a VPO for $\mathcal{N}[u,v]$ but not for $\mathcal{N}$. By definition, if such an arc a exists, then there is a path p in $\mathcal{P}_{\mathcal{N}}$ from $\mathbf{r}_{\mathcal{N}}$ to $\mathbf{t}_{\mathcal{N}}$ containing a such that $w(p) \in \mathtt{PF}\,(\mathcal{N})$; additionally, $\mathcal{P}_{\mathcal{N}}$ shall not contain any other path p'' in $\mathcal{P}_{\mathcal{N}}$ such that $w(p'') \succ w(p)$.

Since $a \in \mathcal{A}_{\mathcal{N}[u,v]}$, and u and v are isolating, p must traverse u and v. Let p' be the subpath of p directed from u to v. Additionally, let p^1 be the portion of p from $\mathbf{r}_{\mathcal{N}}$ to u, and let p^2 be the portion of p from v to $\mathbf{t}_{\mathcal{N}}$. As the removal of a from $\mathcal{N}[u,v]$ does not alter $\mathtt{PF}\,(\mathcal{N}[u,v])$, there must exist a path p'' from u to v for which $w(p') \prec w(p'')$. Let $\tilde{p}$ be the path in $\mathcal{N}$ constructed from concatenating p^1, p'', and p^2. Then, $w(\tilde{p}) \succ w(p)$ (as $w(\tilde{p}) \neq w(p)$ by assumption), which contradicts that $w(p) \in \mathtt{PF}\,(\mathcal{N})$. $\square$

B   Recursive Model Example

$$\mathcal{X} = \{x \in \mathbb{B}^7 \;:\; x_1 + x_2 + x_3 \leq 1, x_2 + x_3 + x_4 \leq 1, x_4 + x_5 \leq 1, x_4 + x_6 \leq 1, x_5 + x_7 \leq 1, x_6 + x_7 \leq 1\}.$$
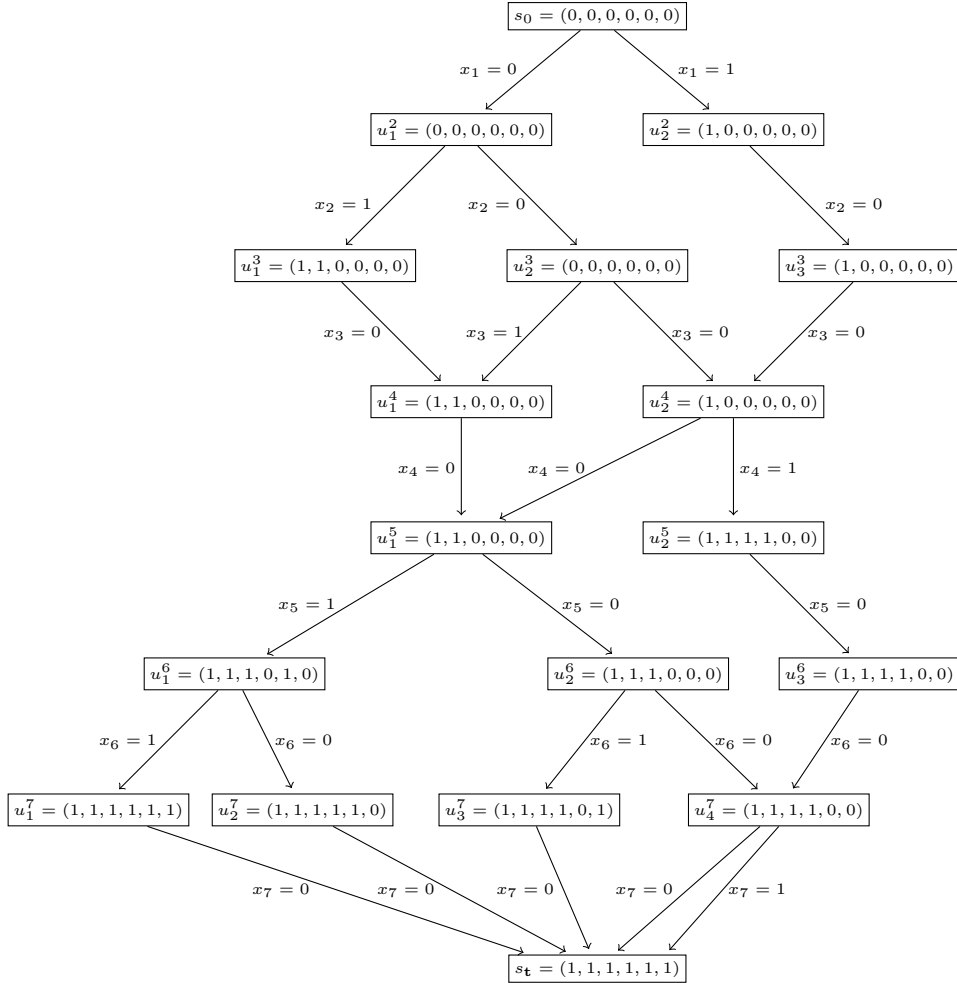
Figure 15: A valid network model for $\mathcal{M}$ in Example 1 obtained by recursive formulation given in Example 3.

28

C Data Generation

Multiobjective 0-1 Knapsack Problem. We experimented on 450 instances of the knapsack problem with $K \in \{3, 4, \ldots, 7\}$ and $n \in \{20, 30, \ldots, 100\}$. Instances were generated as in Kirlik and Sayın (2014): each profit p_j^k and weight w_j was randomly draw from the interval $[1, 1000]$, for $j \in [n]$ and $k \in [K]$. The capacity of the knapsack was set to $W := \lceil 0.5 \sum_{i=1}^{n} w_i \rceil$. Ten instances were generated for each (n, K) pair.

Multiobjective Set Covering and Set Partitioning Problems. We generated 150 random instances based on the previous work by Stidsen et al. (2014). Specifically, we considered $n \in \{100, 150, 200\}$ variables, $m = n/5$ constraints, and fixed 10 variables per constraint (i.e., for every $k = 1, \ldots, m$, we pick 10 elements of the k-th row of A to be 1 uniformly at random). We considered $K = 3, \ldots, 7$ objectives. We sampled 10 instances per (n, K) pair. Each matrix was used both for the MSCP and the MSPP by selecting the appropriate inequality direction in the ensuing constraint system.

Multiobjective Traveling Salesperson Problem. We experimented on 150 instances with $n \in \{5, 10, 15\}$ vertices and $K \in \{3, 4, 5, 6, 7\}$. These instances are generated as in Özpeynirci and Köksalan (2010): for each K, we generated integer coordinates for n cities on a 1000×1000 square (uniformly at random) and used Euclidean distances to create the distance matrix.

Multiobjective Cardinality-Constrained Absolute Value Problem. We experimented on 6,250 instances of the problem. Each was randomly generated with $K \in \{3, 4, 5, 6, 7\}$ and $n \in \{5, 10, 15, 20, 25\}$. For all $k \in [K]$, we drew the components of a^k uniformly at random from the set $[-M, M]$, where we considered $M \in \{50, 100, 150, 200, 250\}$. We let $b_k = \lfloor \mathbf{1}^\top a^k / 2 \rfloor$ for all $k \in [K]$. For the cardinality constraints, we let $C = \lfloor n\delta \rfloor$ for which we considered $\delta \in \{0.1, 0.2, 0.3, 0.4, 0.5\}$.

D Detailed Computational Results

In this section we provide a comprehensive reporting of the computational results. Each line in each table presents the aggregated results of instances whose dimensions are described in the leftmost column: n indicates the number of variables and K gives the number of objective functions. The other columns are arranged in groups of three and present the results for the algorithm indicated on the top. Column S gives the number of instances that were solved within the predefined memory and time limits, and $\bar{t}$ is the average runtime of the algorithm to solve these instances. Column $(\texttt{M}, \texttt{T})$ report pairs (m, t), indicating that the algorithm could not solve m and t instances of that particular configuration because it exceeded the predefined memory and time limits, respectively.

Table 2: Knapsack results

n	K	K S	K $\bar{t}$	K (M,T)	O S	O $\bar{t}$	O (M,T)	TD S	TD $\bar{t}$	TD (M,T)	BU S	BU $\bar{t}$	BU (M,T)	Coup S	Coup $\bar{t}$	Coup (M,T)	TD⁺ S	TD⁺ $\bar{t}$	TD⁺ (M,T)	BU⁺ S	BU⁺ $\bar{t}$	BU⁺ (M,T)	Coup⁺ S	Coup⁺ $\bar{t}$	Coup⁺ (M,T)
20	3	10	0.93	(0,0)	10	1.26	(0,0)	10	0.02	(0,0)	10	0.02	(0,0)	10	0.02	(0,0)	10	0.02	(0,0)	10	0.02	(0,0)	10	0.02	(0,0)
20	4	10	34.41	(0,0)	10	61.45	(0,0)	10	0.03	(0,0)	10	0.03	(0,0)	10	0.03	(0,0)	10	0.02	(0,0)	10	0.03	(0,0)	10	0.03	(0,0)
20	5	6	200.79	(0,4)	8	766.91	(0,2)	10	0.03	(0,0)	10	0.03	(0,0)	10	0.03	(0,0)	10	0.03	(0,0)	10	0.03	(0,0)	10	0.03	(0,0)
20	6	0	-	(2,8)	0	-	(2,8)	10	0.03	(0,0)	10	0.04	(0,0)	10	0.03	(0,0)	10	0.03	(0,0)	10	0.03	(0,0)	10	0.02	(0,0)
20	7	0	-	(0,10)	0	-	(0,10)	10	0.04	(0,0)	10	0.07	(0,0)	10	0.04	(0,0)	10	0.05	(0,0)	10	0.05	(0,0)	10	0.04	(0,0)
30	3	10	5.22	(0,0)	10	6.98	(0,0)	10	0.14	(0,0)	10	0.22	(0,0)	10	0.16	(0,0)	10	0.13	(0,0)	10	0.21	(0,0)	10	0.13	(0,0)
30	4	10	676.25	(0,0)	10	452.18	(0,0)	10	0.18	(0,0)	10	0.53	(0,0)	10	0.2	(0,0)	10	0.18	(0,0)	10	0.54	(0,0)	10	0.18	(0,0)
30	5	0	-	(1,9)	0	-	(0,10)	10	0.3	(0,0)	10	1.42	(0,0)	10	0.34	(0,0)	10	0.38	(0,0)	10	1.27	(0,0)	10	0.26	(0,0)
30	6	0	-	(0,10)	0	-	(0,10)	10	0.72	(0,0)	10	4.78	(0,0)	10	0.87	(0,0)	10	0.97	(0,0)	10	4.22	(0,0)	10	0.5	(0,0)
30	7	0	-	(0,10)	0	-	(0,10)	10	1.75	(0,0)	10	6.24	(0,0)	10	1.63	(0,0)	10	2.8	(0,0)	10	5.25	(0,0)	10	0.97	(0,0)
40	3	10	22.07	(0,0)	10	30.81	(0,0)	10	0.67	(0,0)	10	1.69	(0,0)	10	0.64	(0,0)	10	0.66	(0,0)	10	1.64	(0,0)	10	0.52	(0,0)
40	4	4	1685.96	(0,6)	5	1988.99	(0,5)	10	3.22	(0,0)	10	20.57	(0,0)	10	3.16	(0,0)	10	3.79	(0,0)	10	20.42	(0,0)	10	1.88	(0,0)
40	5	0	-	(1,9)	0	-	(0,10)	10	11.66	(0,0)	10	46.41	(0,0)	10	8.05	(0,0)	10	16.54	(0,0)	10	40.95	(0,0)	10	4.44	(0,0)
40	6	0	-	(0,10)	0	-	(0,10)	10	37.16	(0,0)	10	251.22	(0,0)	10	39.25	(0,0)	10	55.53	(0,0)	10	240.71	(0,0)	10	20.83	(0,0)
40	7	0	-	(0,10)	0	-	(0,10)	10	89.58	(0,0)	9	281.21	(0,1)	10	86.99	(0,0)	10	130.27	(0,0)	9	250.89	(0,1)	10	63.02	(0,0)
50	3	10	36.97	(0,0)	10	52.2	(0,0)	10	2.25	(0,0)	10	5.17	(0,0)	10	1.71	(0,0)	10	2.17	(0,0)	10	5.33	(0,0)	10	1.52	(0,0)
50	4	0	-	(0,10)	2	2841.42	(0,8)	10	23.46	(0,0)	10	134.57	(0,0)	10	11.04	(0,0)	10	28.59	(0,0)	10	125.92	(0,0)	10	6.74	(0,0)
50	5	0	-	(0,10)	0	-	(0,10)	10	110.5	(0,0)	10	1122.29	(0,0)	10	64.76	(0,0)	10	136.59	(0,0)	10	996.69	(0,0)	10	38.8	(0,0)
50	6	0	-	(1,9)	0	-	(0,10)	9	484.95	(0,1)	5	1305.47	(0,5)	10	507.23	(0,0)	9	724.16	(0,1)	5	1249.05	(0,5)	10	400.63	(0,0)
50	7	0	-	(0,10)	0	-	(0,10)	9	1737.94	(0,1)	2	1654.82	(0,8)	9	1195.03	(0,1)	6	1514.52	(0,4)	2	1716.35	(0,8)	10	971.73	(0,0)
60	3	10	107.96	(0,0)	10	143.68	(0,0)	10	9.04	(0,0)	10	25.51	(0,0)	10	4.6	(0,0)	10	9.07	(0,0)	10	23.45	(0,0)	10	3.97	(0,0)
60	4	0	-	(0,10)	0	-	(0,10)	10	169.13	(0,0)	10	792.27	(0,0)	10	51.03	(0,0)	10	191.15	(0,0)	10	784.7	(0,0)	10	34.05	(0,0)
60	5	0	-	(1,9)	0	-	(0,10)	8	1439.71	(0,2)	2	2158.86	(0,8)	10	601.92	(0,0)	6	1007.89	(0,4)	1	834.29	(0,9)	10	416.31	(0,0)
60	6	0	-	(1,9)	0	-	(0,10)	6	2722.71	(0,4)	0	-	(0,10)	6	1389.04	(0,4)	2	1900.28	(0,8)	0	-	(0,10)	7	1124.37	(0,3)
60	7	0	-	(0,10)	0	-	(0,10)	1	2762.75	(0,9)	0	-	(0,10)	3	2454.84	(0,7)	0	-	(0,10)	0	-	(0,10)	5	2174.34	(0,5)
70	3	10	271.77	(0,0)	10	340.95	(0,0)	10	28.85	(0,0)	10	125.02	(0,0)	10	11.85	(0,0)	10	28.43	(0,0)	10	126.12	(0,0)	10	9.08	(0,0)
70	4	0	-	(0,10)	0	-	(0,10)	10	1092.52	(0,0)	4	1605.46	(0,6)	10	257.09	(0,0)	9	903.07	(0,1)	4	1556.9	(0,6)	10	163.71	(0,0)
70	5	0	-	(1,9)	0	-	(0,10)	2	3419.18	(0,8)	0	-	(0,10)	6	2052.85	(0,4)	0	-	(0,10)	0	-	(0,10)	8	1554.53	(0,2)
70	6	0	-	(0,10)	0	-	(0,10)	0	-	(0,10)	0	-	(0,10)	2	1998.62	(0,8)	0	-	(0,10)	0	-	(0,10)	2	1165.76	(0,8)
70	7	0	-	(1,9)	0	-	(0,10)	0	-	(0,10)	0	-	(0,10)	1	3338.91	(0,9)	0	-	(0,10)	0	-	(0,10)	2	2254.76	(0,8)
80	3	10	401.49	(0,0)	10	489.45	(0,0)	10	95.62	(0,0)	10	356	(0,0)	10	29.46	(0,0)	10	98.89	(0,0)	10	351.56	(0,0)	10	23.84	(0,0)
80	4	0	-	(0,10)	0	-	(0,10)	4	846.36	(0,6)	1	2285.8	(0,9)	10	997.93	(0,0)	4	912.5	(0,6)	1	2396.79	(0,9)	10	1012.99	(0,0)
80	5	0	-	(3,7)	0	-	(0,10)	0	-	(0,10)	0	-	(0,10)	4	2676.08	(0,6)	0	-	(0,10)	0	-	(0,10)	4	2225.35	(0,6)
80	6	0	-	(0,10)	0	-	(0,10)	0	-	(0,10)	0	-	(0,10)	0	-	(0,10)	0	-	(0,10)	0	-	(1,9)	0	-	(0,10)
80	7	0	-	(0,10)	0	-	(0,10)	0	-	(0,10)	0	-	(0,10)	0	-	(0,10)	0	-	(0,10)	0	-	(1,9)	0	-	(0,10)
90	3	10	778.15	(0,0)	10	850.51	(0,0)	10	283.73	(0,0)	10	748.69	(0,0)	10	71.74	(0,0)	10	289.5	(0,0)	10	750.2	(0,0)	10	59.84	(0,0)
90	4	0	-	(0,10)	0	-	(0,10)	1	2421.44	(0,9)	0	-	(0,10)	7	1597.38	(0,3)	1	2720.16	(0,9)	0	-	(0,10)	8	1499.22	(0,2)
90	5	0	-	(3,7)	0	-	(0,10)	0	-	(0,10)	0	-	(0,10)	0	-	(0,10)	0	-	(0,10)	0	-	(0,10)	0	-	(0,10)
90	6	0	-	(0,10)	0	-	(0,10)	0	-	(0,10)	0	-	(0,10)	0	-	(0,10)	0	-	(0,10)	0	-	(1,9)	0	-	(0,10)
90	7	0	-	(0,10)	0	-	(0,10)	0	-	(0,10)	0	-	(0,10)	0	-	(0,10)	0	-	(0,10)	0	-	(1,9)	0	-	(0,10)
100	3	8	1631.27	(0,2)	8	1530.55	(0,2)	10	967.47	(0,0)	7	1684.11	(0,3)	10	262.53	(0,0)	10	1048.7	(0,0)	7	1688.68	(0,3)	10	212.64	(0,0)
100	4	0	-	(2,8)	0	-	(0,10)	0	-	(0,10)	0	-	(0,10)	1	745.24	(0,9)	0	-	(0,10)	0	-	(0,10)	2	1764.28	(0,8)
100	5	0	-	(2,8)	0	-	(0,10)	0	-	(0,10)	0	-	(0,10)	0	-	(0,10)	0	-	(0,10)	0	-	(0,10)	0	-	(0,10)
100	6	0	-	(2,8)	0	-	(0,10)	0	-	(0,10)	0	-	(0,10)	0	-	(0,10)	0	-	(0,10)	0	-	(0,10)	0	-	(0,10)
100	7	0	-	(0,10)	0	-	(0,10)	0	-	(0,10)	0	-	(0,10)	0	-	(0,10)	0	-	(0,10)	0	-	(3,7)	0	-	(0,10)

Table 3: Set covering results

		K			O			TD			BU			Coup		
n	K	S	$\bar{t}$	(M, T)	S	$\bar{t}$	(M, T)	S	$\bar{t}$	(M, T)	S	$\bar{t}$	(M, T)	S	$\bar{t}$	(M, T)
100	3	10	8.33	(0,0)	10	10.81	(0,0)	10	10.14	(0,0)	10	10.34	(0,0)	10	10.18	(0,0)
100	4	10	326.36	(0,0)	10	427.21	(0,0)	10	10.7	(0,0)	10	11.32	(0,0)	10	10.61	(0,0)
100	5	1	105.35	(0,9)	1	553.49	(0,9)	10	11.27	(0,0)	10	15.26	(0,0)	10	10.82	(0,0)
100	6	0	-	(0,10)	0	-	(0,10)	10	11.91	(0,0)	10	35.35	(0,0)	10	11.17	(0,0)
100	7	0	-	(0,10)	0	-	(0,10)	10	24.09	(0,0)	10	54.9	(0,0)	10	16.01	(0,0)
150	3	10	34.6	(0,0)	10	44.22	(0,0)	10	36.82	(0,0)	10	59.11	(0,0)	10	36.27	(0,0)
150	4	7	1290.86	(0,3)	9	1485.95	(0,1)	10	83.76	(0,0)	8	197.08	(0,2)	9	62.88	(0,1)
150	5	0	-	(0,10)	0	-	(0,10)	7	196.1	(0,3)	5	652.01	(0,5)	7	136.13	(0,3)
150	6	0	-	(0,10)	0	-	(0,10)	8	539.84	(0,2)	5	803.55	(0,5)	9	315.13	(0,1)
150	7	0	-	(0,10)	0	-	(0,10)	4	783.5	(0,6)	3	1392.27	(0,7)	4	454.3	(1,5)
200	3	10	97.47	(0,0)	10	124.17	(0,0)	1	63.42	(0,9)	1	202.83	(0,9)	1	158.17	(0,9)
200	4	0	-	(0,10)	0	-	(0,10)	1	292.97	(0,9)	0	-	(0,10)	0	-	(0,10)
200	5	0	-	(2,8)	0	-	(0,10)	0	-	(0,10)	0	-	(0,10)	0	-	(0,10)
200	6	0	-	(0,10)	0	-	(0,10)	0	-	(0,10)	0	-	(0,10)	0	-	(0,10)
200	7	0	-	(0,10)	0	-	(0,10)	0	-	(0,10)	0	-	(0,10)	0	-	(0,10)

Table 4: Set packing results

		K			O			TD			BU			Coup		
n	K	S	$\bar{t}$	(M, T)	S	$\bar{t}$	(M, T)	S	$\bar{t}$	(M, T)	S	$\bar{t}$	(M, T)	S	$\bar{t}$	(M, T)
100	3	10	9.38	(0,0)	10	14.34	(0,0)	10	0.09	(0,0)	10	0.12	(0,0)	10	0.08	(0,0)
100	4	10	518.46	(0,0)	10	954.85	(0,0)	10	0.15	(0,0)	10	0.23	(0,0)	10	0.13	(0,0)
100	5	0	-	(0,10)	0	-	(0,10)	10	0.28	(0,0)	10	0.56	(0,0)	10	0.24	(0,0)
100	6	0	-	(0,10)	0	-	(0,10)	10	0.77	(0,0)	10	0.86	(0,0)	10	0.57	(0,0)
100	7	0	-	(0,10)	0	-	(0,10)	10	3.6	(0,0)	10	3.73	(0,0)	10	1.28	(0,0)
150	3	10	23.21	(0,0)	10	36.33	(0,0)	10	12.11	(0,0)	10	17.94	(0,0)	10	12.41	(0,0)
150	4	1	2916.26	(0,9)	2	3057.22	(0,8)	10	27.97	(0,0)	10	75.58	(0,0)	10	23.16	(0,0)
150	5	0	-	(2,8)	0	-	(0,10)	10	87.74	(0,0)	5	155.74	(0,5)	10	65.68	(0,0)
150	6	0	-	(1,9)	0	-	(0,10)	10	203.97	(0,0)	5	318.31	(0,5)	10	125.62	(0,0)
150	7	0	-	(0,10)	0	-	(0,10)	10	888.75	(0,0)	2	196.25	(0,8)	10	475.53	(0,0)
200	3	10	76.47	(0,0)	10	111.18	(0,0)	1	121.92	(0,9)	0	-	(0,10)	1	137.78	(0,9)
200	4	0	-	(0,10)	0	-	(0,10)	0	-	(0,10)	0	-	(0,10)	1	336.82	(0,9)
200	5	0	-	(0,10)	0	-	(0,10)	0	-	(0,10)	0	-	(0,10)	0	-	(0,10)
200	6	0	-	(1,9)	0	-	(0,10)	0	-	(0,10)	0	-	(0,10)	0	-	(0,10)
200	7	0	-	(0,10)	0	-	(0,10)	0	-	(0,10)	0	-	(0,10)	0	-	(0,10)

Table 5: Absolute value results

n	K	C	K			O			TD			BU			Coup		
			S	$\bar{t}$	(M,T)	S	$\bar{t}$	(M,T)	S	$\bar{t}$	(M,T)	S	$\bar{t}$	(M,T)	S	$\bar{t}$	(M,T)
15	3	30	10	1.21	(0,0)	10	1.71	(0,0)	10	0	(0,0)	10	0	(0,0)	10	0	(0,0)
15	4	30	10	8.31	(0,0)	10	25.9	(0,0)	10	0	(0,0)	10	0	(0,0)	10	0	(0,0)
15	5	30	4	1882.3	(0,6)	9	2166.9	(0,1)	10	0	(0,0)	10	0	(0,0)	10	0	(0,0)
15	6	30	0	-	(1,9)	0	-	(1,9)	10	0	(0,0)	10	0	(0,0)	10	0	(0,0)
15	7	30	0	-	(0,10)	0	-	(0,10)	10	0	(0,0)	10	0	(0,0)	10	0	(0,0)
15	3	40	10	2.05	(0,0)	10	2.85	(0,0)	10	0.01	(0,0)	10	0.01	(0,0)	10	0.01	(0,0)
15	4	40	10	23.02	(0,0)	10	65.87	(0,0)	10	0.01	(0,0)	10	0.01	(0,0)	10	0.01	(0,0)
15	5	40	0	-	(0,10)	0	-	(0,10)	10	0.01	(0,0)	10	0.01	(0,0)	10	0.01	(0,0)
15	6	40	0	-	(1,9)	0	-	(1,9)	10	0.02	(0,0)	10	0.02	(0,0)	10	0.02	(0,0)
15	7	40	0	-	(0,10)	0	-	(0,10)	10	0.04	(0,0)	10	0.04	(0,0)	10	0.04	(0,0)
15	3	50	10	2.76	(0,0)	10	3.71	(0,0)	10	0.01	(0,0)	10	0.01	(0,0)	10	0.02	(0,0)
15	4	50	10	31.58	(0,0)	10	87.62	(0,0)	10	0.01	(0,0)	10	0.02	(0,0)	10	0.02	(0,0)
15	5	50	0	-	(1,9)	0	-	(0,10)	10	0.02	(0,0)	10	0.02	(0,0)	10	0.02	(0,0)
15	6	50	0	-	(1,9)	0	-	(0,10)	10	0.03	(0,0)	10	0.04	(0,0)	10	0.03	(0,0)
15	7	50	0	-	(0,10)	0	-	(0,10)	10	0.07	(0,0)	10	0.09	(0,0)	10	0.05	(0,0)
20	3	30	10	7.86	(0,0)	10	9.84	(0,0)	10	0.14	(0,0)	10	0.14	(0,0)	10	0.17	(0,0)
20	4	30	10	89.82	(0,0)	10	222.09	(0,0)	10	0.15	(0,0)	10	0.14	(0,0)	10	0.18	(0,0)
20	5	30	0	-	(1,9)	0	-	(0,10)	10	0.17	(0,0)	10	0.19	(0,0)	10	0.21	(0,0)
20	6	30	0	-	(2,8)	0	-	(0,10)	10	0.24	(0,0)	10	0.28	(0,0)	10	0.29	(0,0)
20	7	30	0	-	(1,9)	0	-	(0,10)	10	0.4	(0,0)	10	0.49	(0,0)	10	0.38	(0,0)
20	3	40	10	32.85	(0,0)	10	40.07	(0,0)	10	0.63	(0,0)	10	0.74	(0,0)	10	0.94	(0,0)
20	4	40	10	553.77	(0,0)	10	1046.7	(0,0)	10	0.7	(0,0)	10	0.76	(0,0)	10	1.06	(0,0)
20	5	40	0	-	(1,9)	0	-	(0,10)	10	0.8	(0,0)	10	0.9	(0,0)	10	1.09	(0,0)
20	6	40	0	-	(0,10)	0	-	(0,10)	10	1.28	(0,0)	10	1.43	(0,0)	10	1.56	(0,0)
20	7	40	0	-	(1,9)	0	-	(0,10)	10	2.62	(0,0)	10	2.67	(0,0)	10	2.41	(0,0)
20	3	50	10	42.55	(0,0)	10	55.92	(0,0)	10	1.37	(0,0)	10	1.56	(0,0)	10	1.98	(0,0)
20	4	50	10	933.77	(0,0)	10	1835.4	(0,0)	10	1.47	(0,0)	10	1.69	(0,0)	10	2.47	(0,0)
20	5	50	0	-	(0,10)	0	-	(0,10)	10	1.84	(0,0)	10	2.15	(0,0)	10	2.78	(0,0)
20	6	50	0	-	(2,8)	0	-	(0,10)	10	3.29	(0,0)	10	3.5	(0,0)	10	3.95	(0,0)
20	7	50	0	-	(0,10)	0	-	(0,10)	10	7.08	(0,0)	10	7.03	(0,0)	10	6.26	(0,0)
25	3	30	10	57.61	(0,0)	10	69.52	(0,0)	10	3.12	(0,0)	10	3.26	(0,0)	10	4.21	(0,0)
25	4	30	10	1209.4	(0,0)	9	2037.7	(0,1)	10	3.35	(0,0)	10	3.59	(0,0)	10	4.43	(0,0)
25	5	30	0	-	(1,9)	0	-	(0,10)	10	3.78	(0,0)	10	3.98	(0,0)	10	5.05	(0,0)
25	6	30	0	-	(0,10)	0	-	(0,10)	10	5.69	(0,0)	10	5.37	(0,0)	10	7.08	(0,0)
25	7	30	0	-	(0,10)	0	-	(0,10)	10	10.54	(0,0)	10	8.97	(0,0)	10	11.03	(0,0)
25	3	40	10	86.15	(0,0)	10	89.88	(0,0)	10	24.76	(0,0)	10	25.68	(0,0)	10	41.76	(0,0)
25	4	40	8	2974	(0,2)	2	3461.5	(0,8)	10	26.58	(0,0)	10	27.51	(0,0)	10	43.84	(0,0)
25	5	40	0	-	(0,10)	0	-	(0,10)	10	32.49	(0,0)	10	33.66	(0,0)	10	51.75	(0,0)
25	6	40	0	-	(0,10)	0	-	(0,10)	10	60.98	(0,0)	10	51.1	(0,0)	10	77.37	(0,0)
25	7	40	0	-	(0,10)	0	-	(0,10)	10	148.45	(0,0)	10	95.4	(0,0)	10	144.34	(0,0)
25	3	50	10	87.75	(0,0)	10	86.78	(0,0)	10	49.21	(0,0)	10	53.73	(0,0)	10	99.72	(0,0)
25	4	50	6	2144.1	(0,4)	2	2135.3	(0,8)	10	54.91	(0,0)	10	60.58	(0,0)	10	106.52	(0,0)
25	5	50	0	-	(0,10)	0	-	(0,10)	10	67.79	(0,0)	10	72.88	(0,0)	10	128.78	(0,0)
25	6	50	0	-	(0,10)	0	-	(0,10)	10	137.12	(0,0)	10	111.41	(0,0)	10	171.18	(0,0)
25	7	50	0	-	(0,10)	0	-	(0,10)	10	427.1	(0,0)	10	222.51	(0,0)	10	358.04	(0,0)